

AD-A056 310

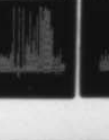
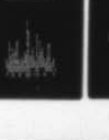
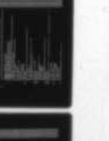
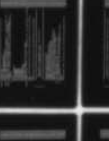
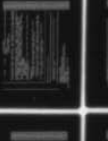
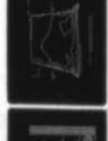
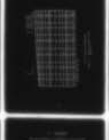
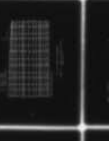
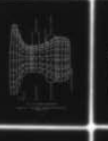
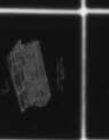
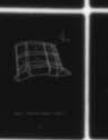
NAVAL POSTGRADUATE SCHOOL MONTEREY CALIF
STRESS ANALYSIS OF CERAMIC TURBINE BLADES BY FINITE ELEMENT MET--ETC(U)
MAR 78 L R EASTERLING
NPS69-78-009

F/G 21/5

UNCLASSIFIED

NL

1 OF 2
AD
A056310





LEVEL III

B.S. **2**

NAVAL POSTGRADUATE SCHOOL
Monterey, California

AD A056310

AD No. **DDC FILE COPY**



DDC
RECEIVED
JUL 18 1978
RECEIVED
D

THESIS

STRESS ANALYSIS OF CERAMIC TURBINE
BLADES BY FINITE ELEMENT METHOD, PART I.

by

Lael Ray Easterling

Mar 1978

12 117 p.

Thesis Advisor:

G. Cantin

Approved for public release; distribution unlimited.

Prepared for: Naval Sea Systems Command
Washington, D. C.
Code 0331

78 07 10 025
257454

SECURITY CLASSIFICATION OF THIS PAGE (When Data Entered)

REPORT DOCUMENTATION PAGE		READ INSTRUCTIONS BEFORE COMPLETING FORM
1. REPORT NUMBER	2. GOVT ACCESSION NO.	3. RECIPIENT'S CATALOG NUMBER
4. TITLE (and Subtitle) Stress Analysis of Ceramic Turbine Blades by Finite Element Method - Part I		5. TYPE OF REPORT & PERIOD COVERED Mechanical Engineer & Master's Thesis; MAR 78
7. AUTHOR(s) Lael Ray Easterling		6. PERFORMING ORG. REPORT NUMBER
9. PERFORMING ORGANIZATION NAME AND ADDRESS Naval Postgraduate School Monterey, California 93940		8. CONTRACT OR GRANT NUMBER(s)
11. CONTROLLING OFFICE NAME AND ADDRESS Naval Postgraduate School Monterey, California 93940		10. PROGRAM ELEMENT, PROJECT, TASK AREA & WORK UNIT NUMBERS N000247WR8G192
14. MONITORING AGENCY NAME & ADDRESS (if different from Controlling Office) Naval Postgraduate School Monterey, California 93940		12. REPORT DATE March 1978
		13. NUMBER OF PAGES
		15. SECURITY CLASS. (of this report) Unclassified
		15a. DECLASSIFICATION/DOWNGRADING SCHEDULE
16. DISTRIBUTION STATEMENT (of this Report) Approved for public release; distribution unlimited.		
17. DISTRIBUTION STATEMENT (of the abstract entered in Block 20, if different from Report)		
18. SUPPLEMENTARY NOTES		
19. KEY WORDS (Continue on reverse side if necessary and identify by block number) Gas Turbine, Stress Analysis, Finite Element; Pre- and Post-Processor.		
20. ABSTRACT (Continue on reverse side if necessary and identify by block number) The search for more efficient gas turbine engines has led to the proposal for the replacement of metal high temperature components with ceramic components. Essential to this effort is the numerical analysis of proposed designs. This thesis report describes the model discretization of a proposed blade design, the development of pre- and post-processors for the ADINA finite element code and the initial stress analysis of the modeled blade.		

DD FORM 1473
1 JAN 73
(Page 1)

EDITION OF 1 NOV 68 IS OBSOLETE
S/N 0102-014-8601

78

SECURITY CLASSIFICATION OF THIS PAGE (When Data Entered)
07 10 025

Approved for public release; distribution unlimited.

Stress Analysis of Ceramic Turbine Blades
by Finite Element Method - Part I

by

Lael Ray Easterling
Lieutenant Commander, United States Navy
B.S., United States Naval Academy, 1968

Submitted in partial fulfillment of the
requirements for the degrees of

MASTER OF SCIENCE IN MECHANICAL ENGINEERING

and

MECHANICAL ENGINEER

from the

NAVAL POSTGRADUATE SCHOOL
March 1978

Author

Lael Ray Easterling

Approved by:

Gillis Cantin

Thesis Advisor

Allen E. Fuhs
Chairman, Department of Mechanical Engineering

George J. Haltiner
Dean of Science and Engineering

ABSTRACT

The search for more efficient gas turbine engines has led to the proposal for the replacement of metal high temperature components with ceramic components. Essential to this effort is the numerical analysis of proposed designs. This thesis report describes the model discretization of a proposed blade design, the development of pre- and post-processors for the ADINA finite element code and the initial stress analysis of the modeled blade.

ACCESSION for	
DTIC	Write Section <input checked="" type="checkbox"/>
DDO	Dist Section <input type="checkbox"/>
UNANNOUNCED	<input type="checkbox"/>
JUSTIFICATION	
BY	
DISTRIBUTION/AVAILABILITY CODES	
Dist.	AVAIL. and/or SPECIAL
A	

TABLE OF CONTENTS

I.	INTRODUCTION -----	10
II.	ANALYTICAL MODEL DEVELOPMENT -----	13
	A. BLADE NOMENCLATURE -----	13
	B. GEOMETRIC DEFINITION -----	14
	1. Airfoil -----	14
	2. Fillet -----	14
	a. Determination of the External Normal -----	15
	b. Locus of 0.3 Inch Radius Centers ---	15
	c. Locus of 0.1 Inch Radius Centers ---	16
	d. Definition of Perimeter Point at Arbitrary Z-Level -----	16
	3. Attachment Root -----	16
	C. ANALYSIS MESH DISCRETIZATION -----	17
III.	PRE-PROCESSOR DEVELOPMENT -----	27
	A. GENERAL DESCRIPTION OF ADINA -----	27
	B. MODIFICATIONS TO ADINA -----	29
	C. CENTRIFUGAL LOADING -----	30
	1. Mathematical Formulation -----	31
	2. Computer Algorithm for Program Centrifugal Load -----	33
	a. Input -----	34
	b. Calculation of Consistent Nodal Loads -----	34
	c. Output -----	34
IV.	PROBLEM SOLUTION -----	37
V.	POST-PROCESSOR DEVELOPMENT -----	38

A.	PROGRAM KCONT -----	39
B.	PROGRAM STRESS -----	40
C.	PROGRAM CONTOUR PLOT DATA -----	40
D.	PROGRAM CONTOUR PLOT -----	41
VI.	RESULTS OF ADINA STRESS ANALYSIS -----	43
A.	COMPARISON OF MAXIMUM PRINCIPAL STRESSES ---	43
B.	CONTOUR PLOT ANALYSIS -----	44
VII.	CONCLUSIONS -----	69
A.	ANALYSIS RESULTS -----	69
B.	OPPORTUNITIES FOR FURTHER RESEARCH -----	70
APPENDIX A	ADDENDUM TO ADINA USER'S MANUAL, REPORT 82448-1, MIT, SEPTEMBER 1975 -----	72
APPENDIX B	CONVERSION OF CALCOMP PLOTTING ROUTINES FOR USE ON A TEKTRONIX 4012 TERMINAL ----	74
APPENDIX C	PROGRAM CENTRIFUGAL LOAD LISTING -----	79
APPENDIX D	PROGRAM KCONT LISTING -----	94
APPENDIX E	PROGRAM STRESS LISTING -----	104
APPENDIX F	PROGRAM CONTOUR PLOT DATA LISTING -----	108
	LIST OF REFERENCES -----	115
	INITIAL DISTRIBUTION LIST -----	117

LIST OF TABLES

1. ADINA PROBLEM SOLUTION TIMES -----	37
2. COMPARISON OF RESULTS OF ANALYSES USING TWO, THREE AND FOUR POINT INTEGRATION -----	44

LIST OF FIGURES

1. Illustration of Nomenclature and Reference System of Turbine Rotor Blade -----	19
2. Illustration of Plane in Which Fillet Geometry is Defined	
Page 1 of 2 -----	20
Page 2 of 2 -----	21
3. Illustration of Plane in Which Attachment Root Geometry is Defined -----	22
4. Airfoil Mesh, Elements 1 through 12 -----	23
5. Attachment Root Mesh	
Page 1 of 2 -----	24
Page 2 of 2 -----	25
6. Completely Assembled Finite Element Analysis Mesh of Proposed Ceramic Gas Turbine Blade Design -----	26
7. Stress Output Locations for ADINA Linear Static Analysis Results -----	36
8. Region of Highest Stress Concentration, Elements 60, 61 and 62 -----	47
9. Attachment Root Finite Element Mesh -----	48
10. Mid-Plane Dovetail Cross-Section	
Page 1 of 3 -----	49
Page 2 of 3 -----	50
Page 3 of 3 -----	51
11. Dovetail Pressure Side	
Page 1 of 3 -----	52
Page 2 of 3 -----	53
Page 3 of 3 -----	54

12.	Dovetail Suction Side	
	Page 1 of 3 -----	55
	Page 2 of 3 -----	56
	Page 3 of 3 -----	57
13.	Level 2.8404	
	Page 1 of 3 -----	58
	Page 2 of 3 -----	59
	Page 3 of 3 -----	60
14.	Level 2.9029	
	Page 1 of 3 -----	61
	Page 2 of 3 -----	62
	Page 3 of 3 -----	63
15.	Level 2.9654	
	Page 1 of 3 -----	64
	Page 2 of 3 -----	65
	Page 3 of 3 -----	66
16.	Maximum Principal Stress Contours for Pressure Side of Airfoil (ksi) -----	67
17.	Maximum Principal Stress Contours for Suction Side of Airfoil (ksi) -----	68

ACKNOWLEDGEMENTS

The author wishes to express his appreciation to the faculty and staff of the Mechanical Engineering Department of the Naval Postgraduate School for their support and motivation throughout his work at this institution. In particular, a great debt of gratitude is owed to Dr. Gilles Cantin, Professor of Mechanical Engineering, for his guidance and friendship as instructor and thesis advisor. Thanks are also extended to the staff of the W. R. Church Computer Center of the Naval Postgraduate School for their invaluable assistance.

Finally, the author thanks his wife, Shay, and daughter, Heather, for their support and forbearance during the demanding period of his academic pursuit.

I. INTRODUCTION

The need to increase fuel efficiency of gas turbines has led to a sizable research investment into suitable materials and designs of ceramic gas turbine components to replace high temperature resistant superalloys. This replacement is envisioned to yield a threefold benefit:

1) The refractory characteristics of ceramics will allow a greater source-sink temperature differential increasing plant efficiency without penalizing overall performance by requiring increased cooling air bled off the compressor.

2) The lower specific weight of ceramics relative to the metal components to be replaced will lower plant weight thereby increasing the plant's power-to-weight ratio.

3) Ceramic constituent components are, in general, domestically available giving them a strategic edge over superalloys.

The basic problem preventing realization of these benefits is the brittle characteristic of ceramics. Since the brittle property is associated with the desirable refractory characteristic, material research and development can only be expected to yield marginally better ceramics in the near future. Any short term success will, therefore, be a result of design innovations which will compensate for the brittle nature of ceramics to allow their use for components which have formerly been engineered on the basis of use of ductile materials.

Essential to this design effort is the use of numerical techniques to model proposed designs and develop alternative criteria with the ultimate goal of minimizing stress concentrations which key catastrophic brittle failure. This thesis describes the efforts of the author to utilize the computer hardware and software available at the Naval Postgraduate School (NPS) to analyze stress distributions in gas turbine ceramic replacement components. Time constraints dictated limiting the scope of analysis to the modeling and development of pre- and post-processors for a proposed first stage ceramic turbine blade subjected to centrifugal loading.

A turbine blade design, developed by the AIRESEARCH division of GARRETT CORPORATION under a Navy managed contract for development of a one-hundred hour test gas turbine engine using ceramic components for the combustor, stator vanes, and rotor blades, was used in this work. Stress distribution analyses were centered around the "Automatic Dynamic Incremental Nonlinear Analysis" (ADINA) code developed by Dr. Klaus-Jurgen Bathe of the Massachusetts Institute of Technology [Ref. 1] as implemented on the NPS IBM 360-67 computer system. The bulk of the modeling effort was accomplished on a Hewlett-Packard 9830 desk top calculator with associated graphics equipment and the PSAP1 graphics package [Ref. 2] implemented on the NPS computer by Lt. Adrian Kibler. Material properties were those of hot-pressed Silicon-Nitride provided by AIRESEARCH. Post-processing graphics utilized a

contour plotting routine developed by Gary L. Giles of Langley Research Center [Ref. 3] and implemented on the NPS computer by Dr. Gilles Cantin of NPS and the author.

The complete analytical efforts were divided into four major categories:

- 1) development of a discretized model of the blade and attachment design.
- 2) development of a pre-processor to calculate consistent centrifugal loads.
- 3) modification of the ADINA code to yield a maximum of stress output locations.
- 4) execution of ADINA with model developed and elaboration of post-processors to help in the interpretation of results.

II. ANALYTICAL MODEL DEVELOPMENT

Developing the finite element mesh of the complex geometric shapes incorporated in the blade was a compromise between geometric accuracy, mathematical compatibility and economy of effort. Using drawings provided by AIRESEARCH [Refs. 4, 5, 6], a mathematical definition of the airfoil and the root was developed separately and then mated using twenty node bricks arranged compatibly throughout the entire assembled mesh.

A. BLADE NOMENCLATURE

Figure 1 illustrates the nomenclature used in this paper to describe the gas turbine blade model and the reference system used to define the geometry. The portion of the component aerodynamically designed to be in the gas flow is termed the airfoil. The fillet is the transition section in between the airfoil and the attachment root designed to minimize stress concentrations. The attachment root (also termed the dovetail) forms the base of the airfoil, provides radial and tangential placement of the blade, and transmits the forces developed by the gas flow to the disk. A right-hand cartesian coordinate system was used to describe the geometry. The X-axis coincided with the turbine axis-of-rotation. The Z-axis coincided with the stacking axis for the airfoil profiles. The Y-axis was then mutually perpendicular to the X- and Z-axis, with the system origin on the rotation axis.

B. GEOMETRIC DEFINITION

1. Airfoil

Reference 4 provided sixty-two perimeter points for x-y plane cross-sections at ten z-levels from $z=3.1$ to $z=4.0$ inches. Linear fairing was prescribed for machining between cross-sections in order to facilitate manufacture. The airfoil tip level of 3.874 inches and z-level 3.385 inches (level of beginning of fillet definition) were plotted and stored for use in discretizing the airfoil. Because of the linear fairing technique, intermediary points were left to the ADINA code feature of node generation for definition.

2. Fillet

The fillet geometry consisted of two radii; 0.3 inch and 0.1 inch. The locus of centers of the 0.3 inch part of the fillet was at a constant level of 3.385 inches. The arc subscribed was tangent to the linear airfoil. The locus of centers of the 0.1 inch radius arc was centered such that the arc subscribed was tangent to both the 0.3 inch radius fillet section and the base which was considered to be a 3.2 inch radius right circular cylinder about the axis of rotation. This double radius design was chosen in order to reduce the possibility of stress concentrations by approximating an elliptic geometry.

Geometric definition of the fillet was made in sixty-two, two-dimensional planes parallel to the Z-axis and containing the normal vector to each of the sixty-two

defined perimeter points at $z=3.385$ inches (Figure 2a). The following described algorithm was developed to define the limiting points illustrated by Figure 2b.

a. Determination of the External Normal

A second degree Lagrange interpolating polynomial was passed through three successive perimeter points at the cross-section $z=3.385$ inches, and the first derivative was evaluated for the middle point in order to determine the slope of the tangent vector at this point. The negative reciprocal of the derivative is the slope of the line normal to the analysis point. Taking the y-component as -1 and the x-component as the derivative (dy/dx), a normal vector was defined. This vector was then normalized to give a unit vector. The analysis point was tested to determine the desired coefficient signs in order to define the normal with the direction external to the body of the airfoil. This procedure was carried out for each perimeter point, thereby defining sixty-two normals from the airfoil.

b. Locus of 0.3 Inch Radius Centers

The coordinate system was translated and rotated to yield a working plane which was parallel to the Z-axis and contained the unit normal vector for the point being analyzed. The curvature center was adjusted in this working plane at $z=3.385$ inches such that the 0.3 inch arc was tangent to the linear airfoil surface. These contact points, defining the start of fillet curvature, were transformed to the original coordinate system for future use.

c. Locus of 0.1 Inch Radius Centers

The 0.1 inch radius curvature centers were defined in each of the sixty-two working planes by use of a Newton iteration scheme to adjust the center of curvature such that the subscribed arc was tangent to both the 0.3 inch arc and the top of the root. These points of tangencies were determined, transformed to the original coordinate system and stored.

d. Definition of Perimeter Point at Arbitrary Z-Level

Using the above determined points (Figure 2b), an algorithm was developed which took as input any desired z-level in the fillet region, tested for the correct definition of geometry for that level and yielded an array of sixty-two perimeter surface points for that level.

Information from the above procedure allowed the definition of a sixty-two point perimeter at any z-level of an airfoil or fillet cross-section parallel to the x-y plane.

3. Attachment Root

The attachment root geometry was defined in a vertical plane containing the stacking axis and perpendicular to the horizontal longitudinal centerline of the body of the root which has a broach angle of 23° relative to the axis of rotation (Figure 3). Nine different geometries consisting of straight lines and arcs of circles were defined by Ref. 6 in this plane for the perimeter of the root. These geometries were mathematically defined, and the limiting point coordinates of each segment were determined. This

shape was projected into the fore and aft faces of the disk. Symmetry conditions allowed simple manipulations of coordinates in order to define the shape of the entire attachment root. An algorithm was developed to define 231 points on any desired horizontal surface.

C. ANALYSIS MESH DISCRETIZATION

Major considerations in the development of the analysis model were to define a mesh which adequately described the geometry of the blade and yielded sufficient data points for meaningful evaluation, without making the mesh so fine as to require an inordinate amount of computer time for solution. Twenty node bricks were chosen for use throughout the mesh because of their capability of accurately defining any second order geometric curve (used almost exclusively by the designers of the blade) and their isotropic sensitivity to the applied loads.

The airfoil was represented by a mesh of twelve elements arranged one deep, three high and four long (Figure 4). The top two layers defined the linearly faired section, and the bottom row defined the fillet region. Choice of nodal point coordinates were made with the assistance of plots of horizontal cross-sections of points defined by geometry definition algorithms.

Chosen for the attachment root representation were nominal three deep, four long layers of elements defining each different vertical geometric segment (Figure 5). The exact

make-up of the root mesh was controlled by the mating of the airfoil with the attachment root which caused significant distortions because the design definition of the fillet base extended beyond the limits of the top surface of the attachment root. This mis-match of geometries necessitated brute force adjustment of nodal point coordinates in order to mate the two regions into a single consistent mesh.

Once the mating process was accomplished, all the chosen nodal points and the element connectivities were card punched in the format required by ADINA. The ADINA deck was then used as input to the PSAP1 graphics package in order to de-bug the mesh. After adjustments were made to yield a visually satisfactory mesh, a trial analysis was run which brought to light numerous mathematical difficulties caused by the distortions resulting from the mating of dissimilar geometries. These were corrected, and the final mesh (Figure 6) was considered ready for analysis.

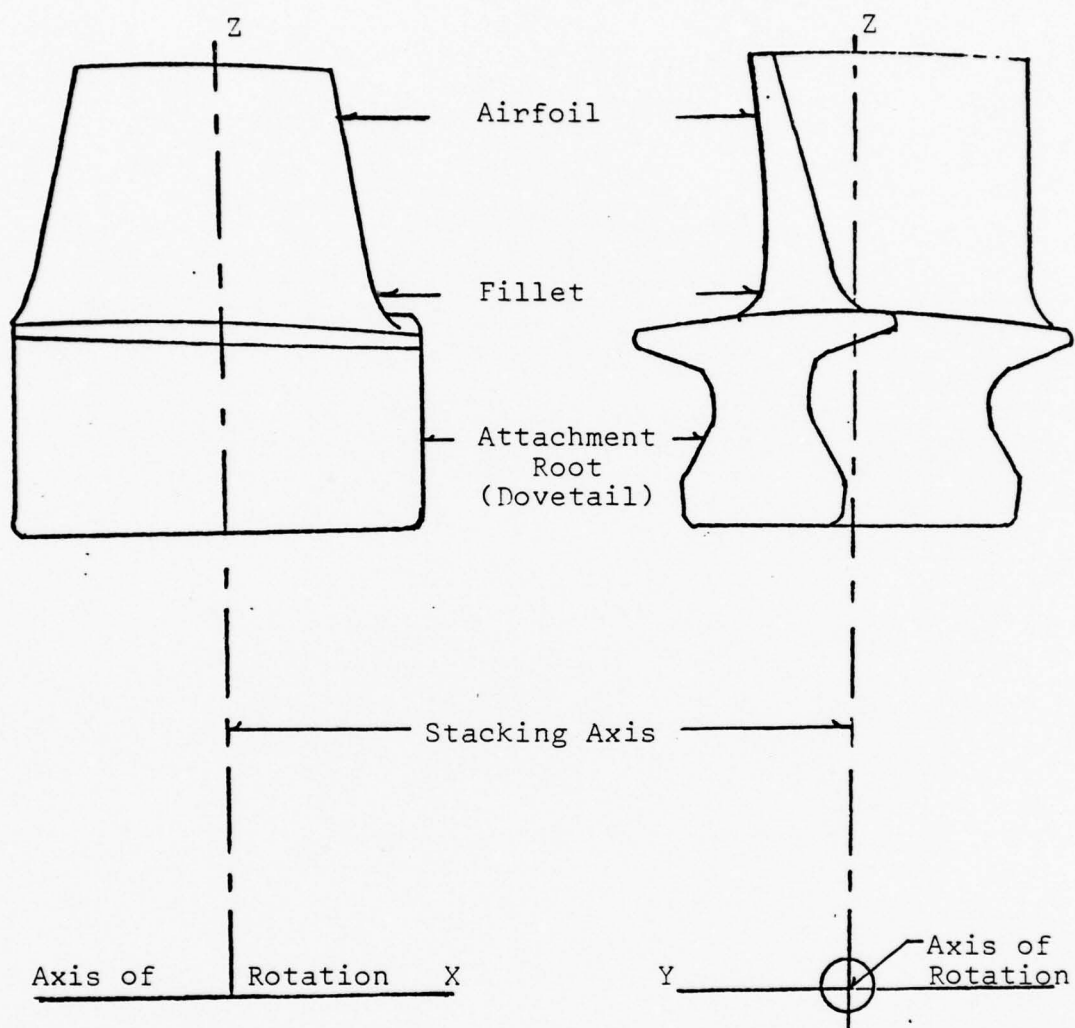
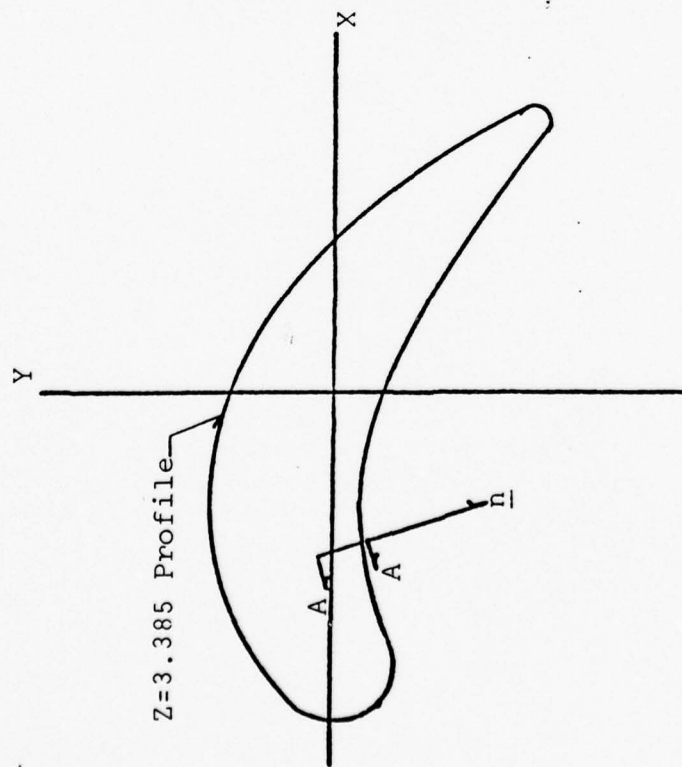
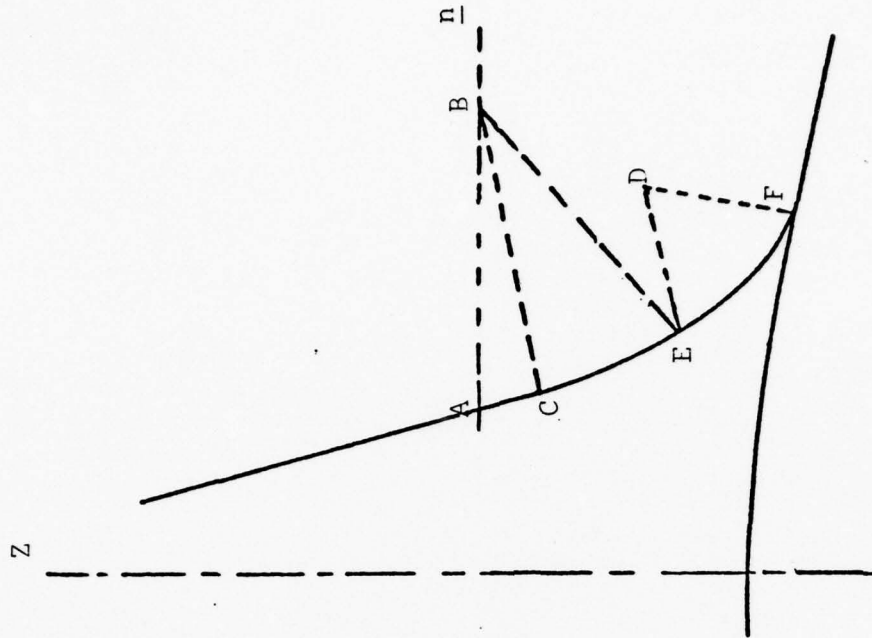


Figure 1. Illustration of Nomenclature and Reference System of Turbine Rotor Blade.



(a)



Section A-A

(b)

Figure 2. Illustration of Plane in Which Fillet Geometry is Defined.
Page 1 of 2

Definition of nomenclature for Figure 2

\underline{n} = outward pointing normal

A = level $z = 3.385$ inches

B = center of 0.3 inch fillet radius curvature

C = point of tangency between linear airfoil and fillet
curvature

D = center of 0.1 inch fillet radius curvature

E = point of tangency between 0.3 inch fillet curvature
and 0.1 inch fillet curvature

F = point of tangency between 0.1 inch fillet curvature
and attachment root surface

Figure 2. Continued, Page 2 of 2.

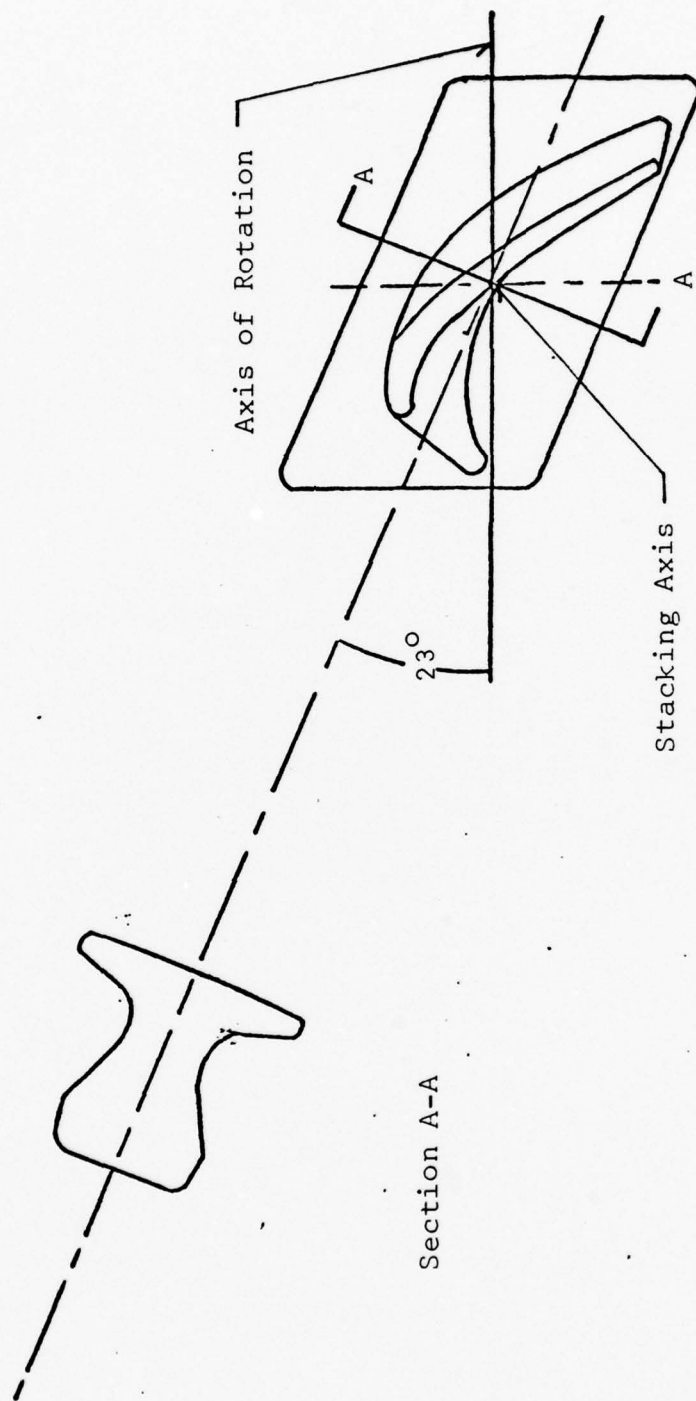


Figure 3. Illustration of Plane in Which Attachment Root Geometry is Defined.

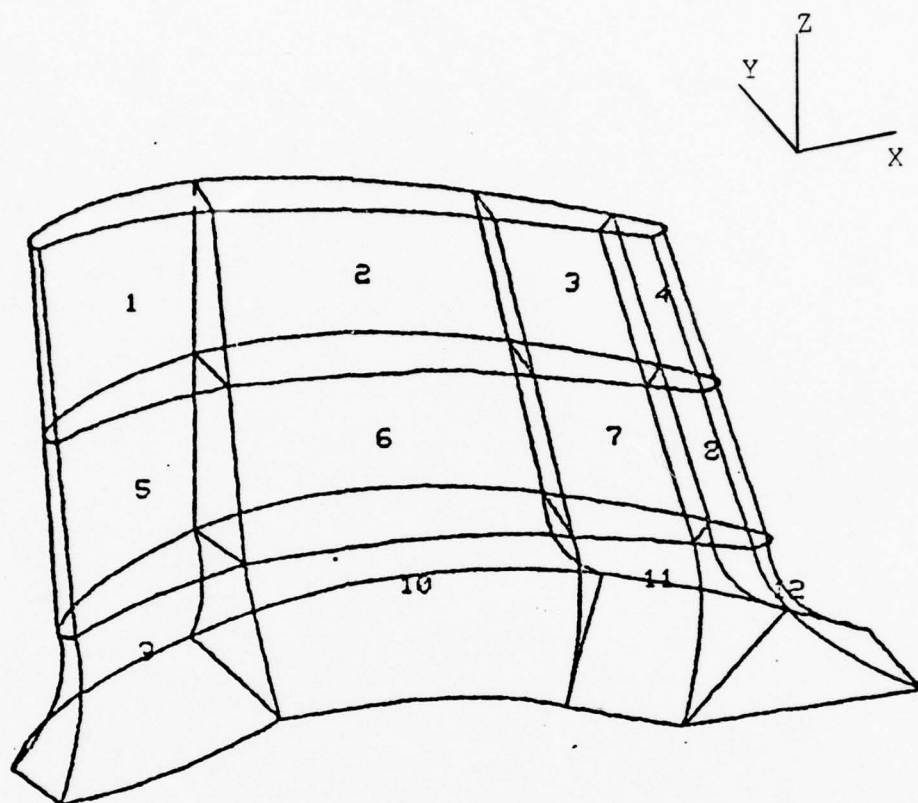
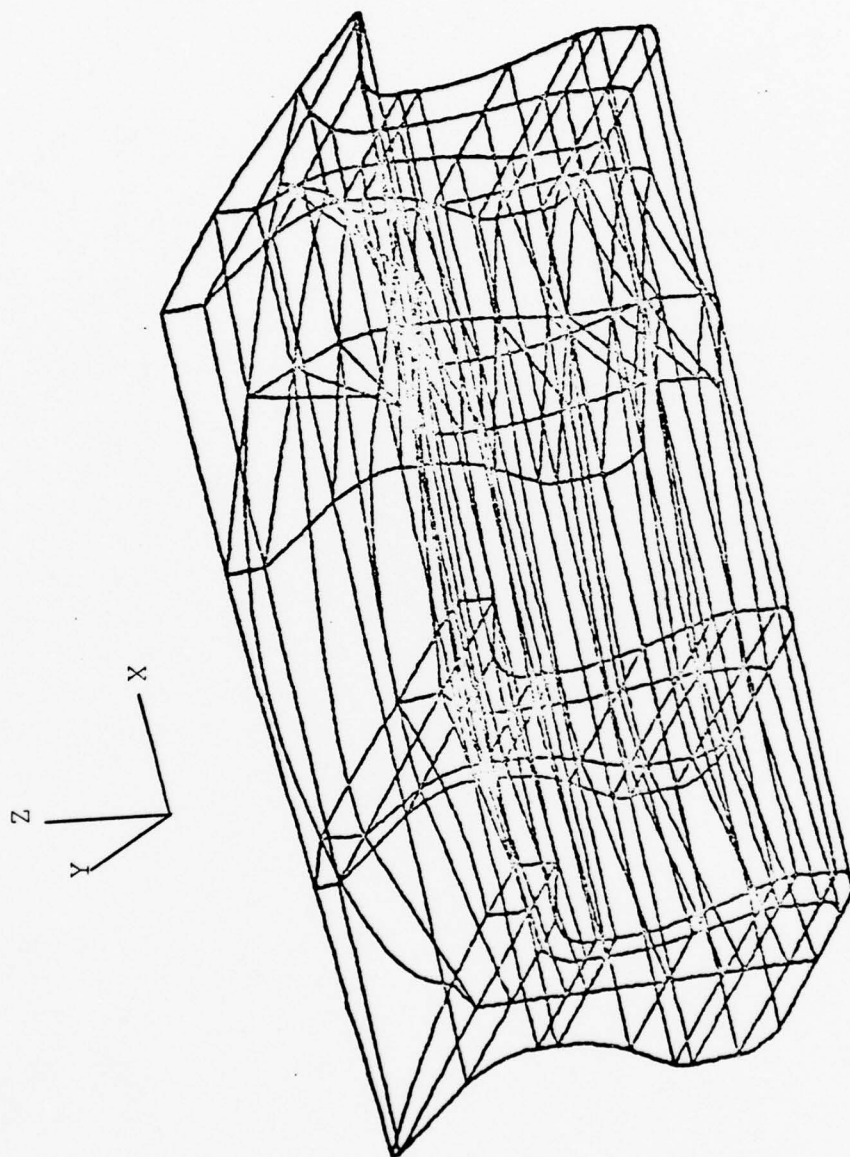
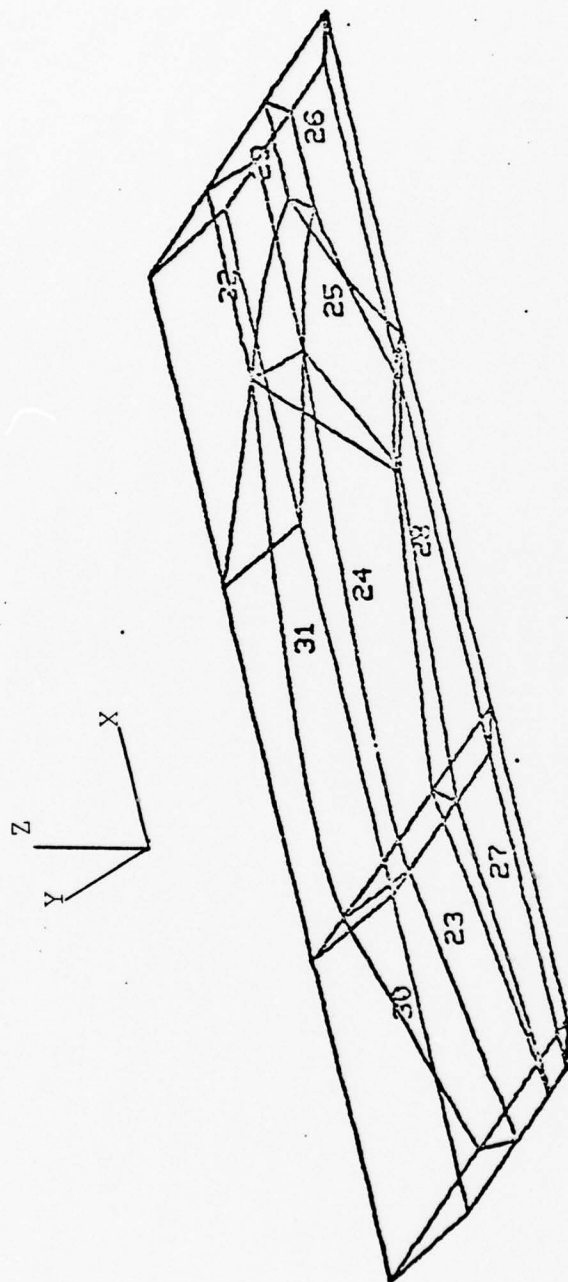


Figure 4. Airfoil Mesh, Elements 1 through 12.



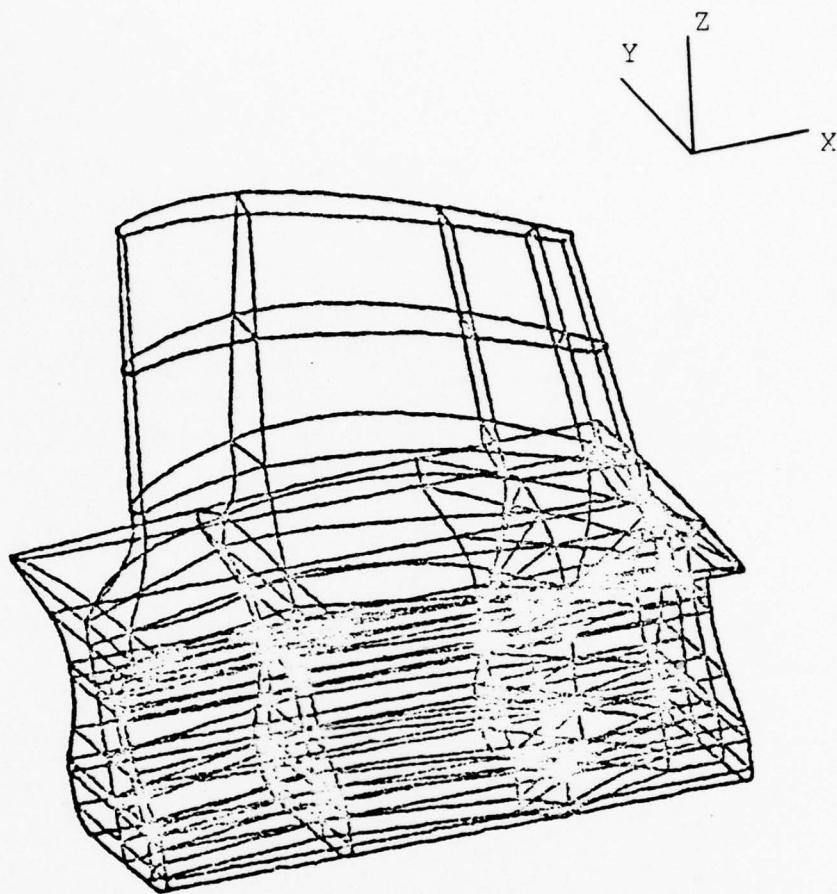
(a) Elements 13 through 102

Figure 5. Attachment Root Mesh,
Page 1 of 2.



(b) Elements 23 through 32

Figure 5. Continued, Page 2 of 2.



EASTERLING-FINITE ELEMENT ANALYSIS
OF A CERAMIC GAS TURBINE BLADE

Figure 6. Completely Assembled Finite Element
Analysis Mesh of Proposed Ceramic Gas
Turbine Blade Design.

III. PRE-PROCESSOR DEVELOPMENT

The ADINA finite element code is a flexible, state-of-the-art code encompassing linear and non-linear, static and dynamic analyses with a choice of six types of elements and twenty material models in various combinations with element types. In this section, an explanation of the facets and capabilities of ADINA used in the blade analysis is given along with a description of the preparations that were necessary prior to execution of an analysis.

A. GENERAL DESCRIPTION OF ADINA

The brittle behavior of the hot-pressed Silicon-Nitride lends itself to the use of the linear isotropic elastic material model. Twenty node isoparametric bricks were used throughout the mesh. ADINA's use of an out-of-core solution scheme and compacted storage of matrices lends itself attractively for analysis of a large mesh which is required for the blade analysis because of the necessity of describing many different geometries.

For the chosen material model and static analysis, the equilibrium equation solved by ADINA is:

$$KU = R$$

where

K = stiffness matrix

U = displacement matrix

R = load matrix

The stiffness matrix is defined as:

$$K = \int_V B^T C B dV$$

where

B = strain-displacement transformation matrix

C = constitutive stress-strain matrix

The elements of B are functions of the natural coordinates r, s, t, being derived from the isoparametric representation of displacements and the inverse of the Jacobian matrix. The integration is carried out in the natural coordinate system of reference, and dV is defined as

$$dV = \det(J) dr ds dt,$$

where $\det(J)$ is the determinant of the Jacobian matrix. Integration is accomplished using Gauss quadrature with the resulting matrix elements being stored in compacted form.

With the exception of gravity loading, concentrated nodal forces are the only allowed force inputs incorporated in the ADINA code implemented on the NPS computer. The rotation induced centrifugal body force needed for this analysis was obtained using an external pre-processor to be discussed in Section III-C.

In ADINA, boundary conditions constraining the structure model are imposed by eliminating global degrees of freedom of selected nodes. The real structure was constrained by a Waspaloy disk with a compliant layer interface between the ceramic contact surface and metal disk. Interpretation of

the behavior of this system of materials varies among investigators with consequent variations in modeling the boundary conditions. Without concise information on the behavior of the actual constraining mechanisms and having to limit the scope of this investigation, the tack taken was to eliminate all degrees of freedom for all nodes defining the blade contact surface.

B. MODIFICATIONS TO ADINA

The ADINA code's complex dynamic dimensioning scheme inhibits the user from making major adjustments, additions or deletions to the implemented code. Two modifications, however, were deemed important enough to implement within the code. Other problem related manipulations were implemented by external algorithms which use the ADINA input deck but do not affect the code.

Originally, ADINA came to a STOP statement when a zero or negative determinant of the Jacobian matrix was encountered. This is a valid procedure since the results of subsequent analysis would be incorrect; however, given the inexperience of this investigator and the distortions of various elements due to the requirement of producing a compatible and complete model, numerous elements were suspected of being ill-behaved, and the STOP procedure prevented efficient troubleshooting. The diagnostic output also inhibited efforts to correct model inadequacies because of a lack of identification of the offending node and element. These problems were circumvented

by deletion of the STOP statement and addition to the diagnostic the location of the offending node and element, allowing identification of all improper elements on a single trial run.

ADINA stress output consisted of three normal and three shear stresses for sixteen nodes out of a possible twenty-seven locations for each element being transmitted solely to the line-printer device. The necessity for meaningful manipulation of the massive output derived from the 682 node mesh and the desire for higher density value coverage for input into contour plotting post-processing dictated modification of the ADINA output capabilities. An additional input parameter was defined in the master control cards which allowed the user the option of requesting output values of all twenty-seven possible output locations (Figure 7). A WRITE statement was inserted to output, on a user defined file 57, all nodal stresses. Appendix A details the changes necessary to the ADINA User's Manual [Ref. 1] resulting from these modifications along with other changes from a companion investigator's contributions.

C. CENTRIFUGAL LOADING

Principal modes of loading considered for the blade were thermal, pressure and centrifugal. Given the temperature distribution, ADINA has the capacity for determining thermal gradient induced loads. External pre-processing was chosen for development of pressure and centrifugal loading. The

pressure loading pre-processor was developed by Lieutenant J. Preisel and reported in Ref. 7. A centrifugal loading algorithm was developed by this author and is described herein.

The ADINA version implemented on the Naval Postgraduate School computer accepts only concentrated nodal forces. An algorithm was developed which would calculate the nodal consistent loads equivalent to a rotation induced body force and produce an output of punched cards in a format acceptable to ADINA.

1. Mathematical Formulation

Starting with Newton's Second Law:

$$\underline{F} + \underline{I} = 0$$

$$\underline{I} = -m \underline{a} = -\int_V \rho dV \underline{a}$$

where

\underline{F} = external forces

\underline{I} = inertia forces

m = mass

ρ = mass density

\underline{a} = acceleration

dV = differential volume

A vector of discretized consistent nodal forces (V_i) is desired such that

$$\langle V_i \rangle \{u_i\} = \langle I \rangle \{u\}$$

where

$\langle V_i \rangle$ = vector of consistent loads

$\{u_i\}$ = vector of discrete displacements

$\langle I \rangle$ = vector of inertia force components I_x, I_y, I_z

$\{u\}$ = vector of displacement function components
 $\langle u, v, w \rangle^T$

Using a right-hand cartesian coordinate system and isoparametric element definitions, displacements and coordinates are discretized by

$$\begin{aligned}\{u\} &= \langle h_i \rangle \{u_i\} \\ \{x\} &= \langle h_i \rangle \{x_i\}\end{aligned}\tag{3}$$

where

$\langle h_i \rangle$ = vector of shape functions = $f(r,s,t)$

$\{x\}$ = continuum coordinates $\langle x,y,z \rangle^T$

$\{x_i\}$ = discrete nodal coordinates

The acceleration matrix is defined by

$$\underline{a} = \underline{w} \times (\underline{w} \times \underline{r})\tag{4}$$

where

\underline{w} = angular velocity vector = $w_x \underline{i} + w_y \underline{j} + w_z \underline{k}$

\underline{r} = position vector = $x \underline{i} + y \underline{j} + z \underline{k}$

\underline{a} = acceleration vector = $a_x \underline{i} + a_y \underline{j} + a_z \underline{k}$

After vector algebra manipulation, one derives

$$\{a\} = [A] \{x^*\}\tag{5}$$

where

$$A = \begin{bmatrix} -(w_y^2 + w_z^2) & w_x w_y & w_x w_z \\ w_x w_y & -(w_z^2 + w_x^2) & w_y w_z \\ w_x w_z & w_y w_z & -(w_x^2 + w_y^2) \end{bmatrix}$$

$$\{a\} = \langle a_x, a_y, a_z \rangle^T$$

$$\{x^*\} = \langle x, y, z \rangle^T$$

Discretizing equations (1) and (5), using equation (3), and substituting into equation (2), one has

$$\langle V_i \rangle \{u_i\} = \rho \int \langle x_i \rangle \{h_i\} [A] \langle h_i \rangle dVol \{u_i\}$$

where

$$dVol = \det J \, dr \, ds \, dt$$

Simplifying and rearranging yield the following equation which was used to program the computer algorithm for development of consistent loads:

$$\{V_i\} = \rho \int \{h_i\} [A] \langle h_i \rangle \{x_i\} \, dVol$$

2. Computer Algorithm for Program Centrifugal Load

The centrifugal load algorithm is generalized for use by any ADINA three-dimensional brick element mesh defined by eight to twenty nodes per element. A dynamic dimensioning scheme is used in order to conserve core and simplify changes dictated by the size of the user's mesh.

a. Input

Angular velocity about the three cartesian axes, mass density and an ADINA input deck are the required input for calculations in Program Centrifugal Load. In addition, several housekeeping parameters are required as defined in Appendix C.

The ADINA input deck provides node coordinates and mesh connectivity. By using the subroutine RDADIN, duplication of the considerable effort to punch and debug a large mesh is obviated. This subroutine should prove very useful for future users of ADINA who wish to manipulate mesh values.

b. Calculation of Consistent Nodal Loads

The user can select two to six Gauss point integration in the calculations of the consistent loads. Shape functions were derived from Ref. 8, which are the same used in ADINA. After calculation of loads for each element, the contributions to each node are summed in each of the three cartesian coordinate directions to yield the desired output of concentrated nodal forces. ADINA has the capability of summing concentrated nodal forces in a common direction for a given node; therefore, loads other than centrifugally induced may be input by the user without necessitating modification to Program Centrifugal Load output.

c. Output

Four options allow the user to restrict the output to what is desired for the particular problem under investigation:

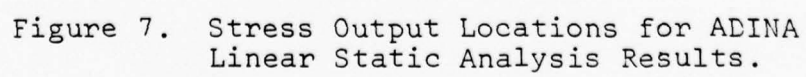
(1) ICLK1. This flag allows the option for printout of the nodal coordinate data and mesh connectivity. Since this data is also output by use of the ADINA code and PSAP1, the user would normally not desire this option from Program Centrifugal Load.

(2) ICLK2. This parameter controls the option for controlling the output of consistent loads calculated for each element. The information may be useful in comparing the contributions of various elements.

(3) ICLK3. The information required by ADINA is controlled by this parameter which allows printout of the totaled consistent loads for each node for the three coordinate directions.

(4) ICLK4. This parameter gives the user the option of not punching the data cards as may be the choice for a first run.

Other output items include the total force in each of the three coordinate directions and the total number of load cards punched. The latter value is required by ADINA as parameter NLOAD on the Load Control Card described in Section IV of Ref. 1.



IV. PROBLEM SOLUTION

The ADINA problem solution was executed for two, three and four Gauss points used for development of the stiffness matrix. Static linear analysis was chosen for the solution method, and a material model for isotropic behavior was used. A Young's modulus of 4.0×10^7 psi was used, corresponding to the approximate value for hot-pressed Silicon-Nitride at 2500°F. Poissons ratio was chosen to be 0.33. Loading was accomplished using concentrated nodal forces with values obtained from the centrifugal load pre-processor for an angular velocity of 42,000 rpm about the X-axis. Table 1 summarizes the execution times for the three analyses.

OPERATION	ORDER OF INTEGRATION		
	2	3	4
INPUT PHASE	22.74	20.83	24.52
MATRICES ASSEMBLAGE	717.19	1437.83	3305.98
TRIANGULARIZATION OF STIFFNESS MATRIX	637.36	663.63	705.98
STEP BY STEP SOLUTION	110.78	111.29	110.11
TOTAL SOLUTION TIME	1549.57	2234.96	4148.07

TABLE 1. ADINA PROBLEM SOLUTION TIMES (seconds)

V. POST-PROCESSOR DEVELOPMENT

Static linear analysis using the modified version of ADINA yields three orthogonal displacements for each input node and three normal and three shear stresses at each of twenty-seven locations in a twenty node brick. The value of the stress components calculated at a given node will, in general, differ from element to element. Experience has shown that the straight average of these values give the best estimate of the real stress at that node [Ref. 8]. For problems involving brittle material, the principal stresses (particularly the maximum principal stresses) are the primary values of concern in predicting failure of the modeled component. These factors necessitated the development of post-processors to manipulate the ADINA output into the values required for analysis of results. The consequent output of these post-processors was still unmanageable from the standpoint of visual perception of the relation of the results with model geometry. Additional post-processors were, therefore, developed to yield the coordinates and connectivity of a twenty-seven node brick mesh and output of punched cards in a format applicable to the contour plotting code implemented on the Naval Postgraduate School computer.

A. PROGRAM KCONT

Prior to data manipulation, the coordinates of all nodes of the twenty-seven node brick mesh and the connectivity must be known. Program KCONT was developed to accomplish this task by using the basic isoparametric finite element model equalities:

$$x = \sum_{i=1}^n h_i x_i$$

$$y = \sum_{i=1}^n h_i y_i$$

$$z = \sum_{i=1}^n h_i z_i$$

where

x, y, z = global coordinates of any point within the element

x_i, y_i, z_i = global coordinates of the nodes defining the element

h_i = the array of shape factors as the function of the natural coordinates r, s, t .

Program KCONT first reads an ADINA input deck. It takes the input node coordinates and mesh connectivity data and computes the coordinates of the additional nodes. The twenty-seven node brick mesh connectivity is assembled and is output along with the coordinates of all nodes to the line printer and to the user defined storage files in accordance with the instructions in Appendix D.

B. PROGRAM STRESS

Program Stress reads the file defined by the ADINA code user for storage of stress results and the files storing the total connectivity and coordinate information, averages all values for each given node and determines the principal stresses from the average values. The output consists of storage of the results on user defined files and a line printer presentation. Refer to Appendix E for instructions on using Program Stress.

C. PROGRAM CONTOUR PLOT DATA

Data required by the two-dimensional iso-line contour plotting code consists of housekeeping information in the form of defined NAMELISTS, coordinate data of nodes on the analysis plane, four-node two-dimensional connectivity and input values of information to be plotted. Program Contour Plot Data was designed to define the desired analysis plane(s) and yield a punched data deck of coordinates and plotting value information. A graphics generated plot of node points and global numbers is also generated to assist the user in the formulation of the connectivity. The connectivity information must then be punched on data cards by the user and inserted into the appropriate data deck location.

Analysis planes can be defined with any of three options. The user can simply input the nodes to be used on data cards in the format 16I5. Most models, however, have surfaces of interest which are parallel to one of the three orthogonal

planes defined by the axes of the right-handed cartesian coordinate systems. Should this be the case, the user may define bounding values of a coordinate for testing the mesh for the desired nodes defining the analysis plane. If the user inputs both bounding values equal, an equality test is made in order to define the desired plane.

The program as written takes the array of plotting values from the file containing the principal stresses established by Program Stress and uses the maximum principal stress array (variable SIGMX) for plotting contours. A user may redefine the read statement (line CTRP2470 of Appendix F) in order to input the desired values for a particular problem, filling the array SIGMX with the desired plotting data. Coordinate values are read from file 58 established by Program KCONT.

The resulting punched deck of cards requires the input of connectivity and NAMELISTS &OPTION and &PICT in locations designated by Ref. 3.

D. PROGRAM CONTOUR PLOT

The contour plotting routine chosen to display stress results was developed by Gary L. Giles of the Langley Research Center for use with a variety of graphic systems including the CALCOMP plotter installed at the Naval Postgraduate School. Unfortunately, the NPS graphics software package rotates the plotting axis 90° clockwise from the original software conception of plot orientation. In order

to achieve optimum utilization of the plotting surface, the decision was made to modify the contour plot routine to utilize the NPS graphics package but yield a plot oriented with the horizontal plotting axis along the length of the paper roll as originally conceived by the CALCOMP manufacturer. In general this requires inputting to the drawing routines of NPS the negative of the desired vertical coordinate in the calling location for the x-coordinate and the positive horizontal coordinate in the calling position of the y-coordinate.

The plotting origin for the analysis plane is chosen to be the geometric center. In order to place the plot properly on the plotting surface for any set of coordinates, parameters PXORGN and PYORGN were added to NAMELIST &OPTION with default values of 0.0. Inputting the user's coordinates for the center of his analysis plane properly centers the plot on the plotting surface.

VI. RESULTS OF ADINA STRESS ANALYSIS

Stress results were analyzed using a program developed to compare the results of the two, three and four point Gauss integration analyses and plotting the iso-maximum principal stress contours for various chosen planes of analysis. Severe surface tensile stress concentrations were observed in the region immediately above the ceramic-disk contact region.

A. COMPARISON OF MAXIMUM PRINCIPAL STRESSES

Formulation of the stiffness matrix using two-point integration resulted in higher stresses caused by a lower order in integration, creating a more flexible system which concurs with finite element research [Ref. 8]. Some investigators have found that the results of reduced order integration reflect more accurately the actual component stresses because the strict mathematical development of the finite element method creates a system which is stiffer than the actual component. Insufficient experimental data, uncertainty of boundary conditions and the lack of an adequate convergence study prevent a statement of qualitative opinion of the actual stresses involved for the blade analysis; however, noting the failure rate of the few specimens which have been tested, it is probable that tensile stresses in the dovetail are higher than predicted.

Table 2 illustrates the differences between the three analyses by comparing the greatest maximum principal stress

encountered, the average of maximum principal stresses and the Euclidean norm of the differences between results for different integration order analysis.

	ORDER OF INTEGRATION		
	2	3	4
MAXIMUM PRINCIPAL STRESS	52862.39	46671.73	4674.73
AVERAGE MAX PRINCIPAL STRESS	6198.79	6100.42	6093.98
INTEGRATION ORDER ANALYSES COMPARED			
	2-3	2-4	3-4
EUCLIDEAN NORM	122.2901	122.6712	4.7777

TABLE 2. COMPARISON OF RESULTS OF ANALYSES USING TWO, THREE AND FOUR POINT INTEGRATION (psi)

The maximum value occurred at node 394 which is located immediately above the contact region at level 2.9029 (Figure 8). Results from the three and four order of integration analyses showed little difference, indicating that the order of integration necessary for the "exact" evaluation of the stiffness matrix elements is being approached.

B. CONTOUR PLOT ANALYSIS

Thirty-four analysis planes were defined for contour plots. Presented herein are eight of these planes which show the regions of highest stress concentrations and the distribution of stresses in the airfoil. Figure 9 illustrates the relative position of the six plots of analysis

planes in the attachment root. The level number refers to the z-coordinate value of the nodes on that plane. The figures presented consist of an element plot, illustrating the coverage of input values to the contour plotting code, and the iso-stress plots from the second and fourth order integration analyses.

Figure 10 shows severe surface stress concentrations on both pressure and suction sides of the dovetail in the region immediately above the blade-disk contact surface. This result is consistent with other analyses of blades of similar design regardless of the boundary conditions used and loading scheme, indicating the stress distribution is principally a function of geometry. The orders of magnitude of the stress concentrations are fifty ksi for the two-point integration plot and forty-five ksi for the four-point integration plot.

Figures 11 and 12 present another view of the vertical stress distribution in dovetail. Noteworthy information from these plots is that the stress concentration is generally uniform along the length of the attachment root.

Figures 13 through 15 are plots of three horizontal surfaces in the region of high stress concentration in the dovetail.

Another region of concern in the design of a ceramic turbine blade was the fillet area of the airfoil. Figures 16 and 17 illustrate the stress distributions in the airfoil as viewed from the pressure and suction sides. Some stress

concentration does occur at the leading and trailing edges at the mid-fillet height; however, the values are minor compared to magnitudes obtained in the attachment root and relative to the strength of the material. Test results to date also indicate the adequacy of the fillet design as no failures have originated in this region except for impact initiated failure caused by flying debris upon failure of other blades.

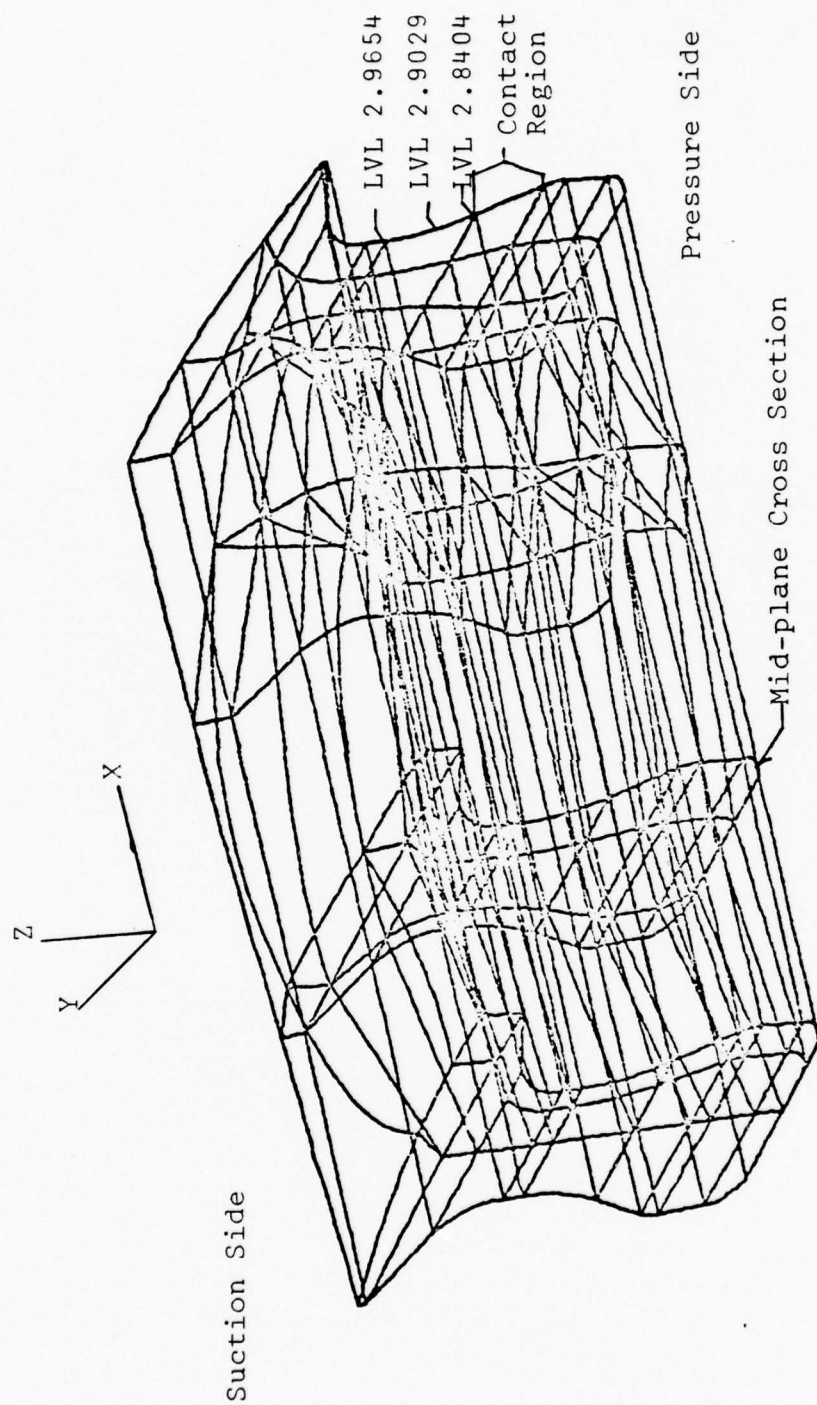
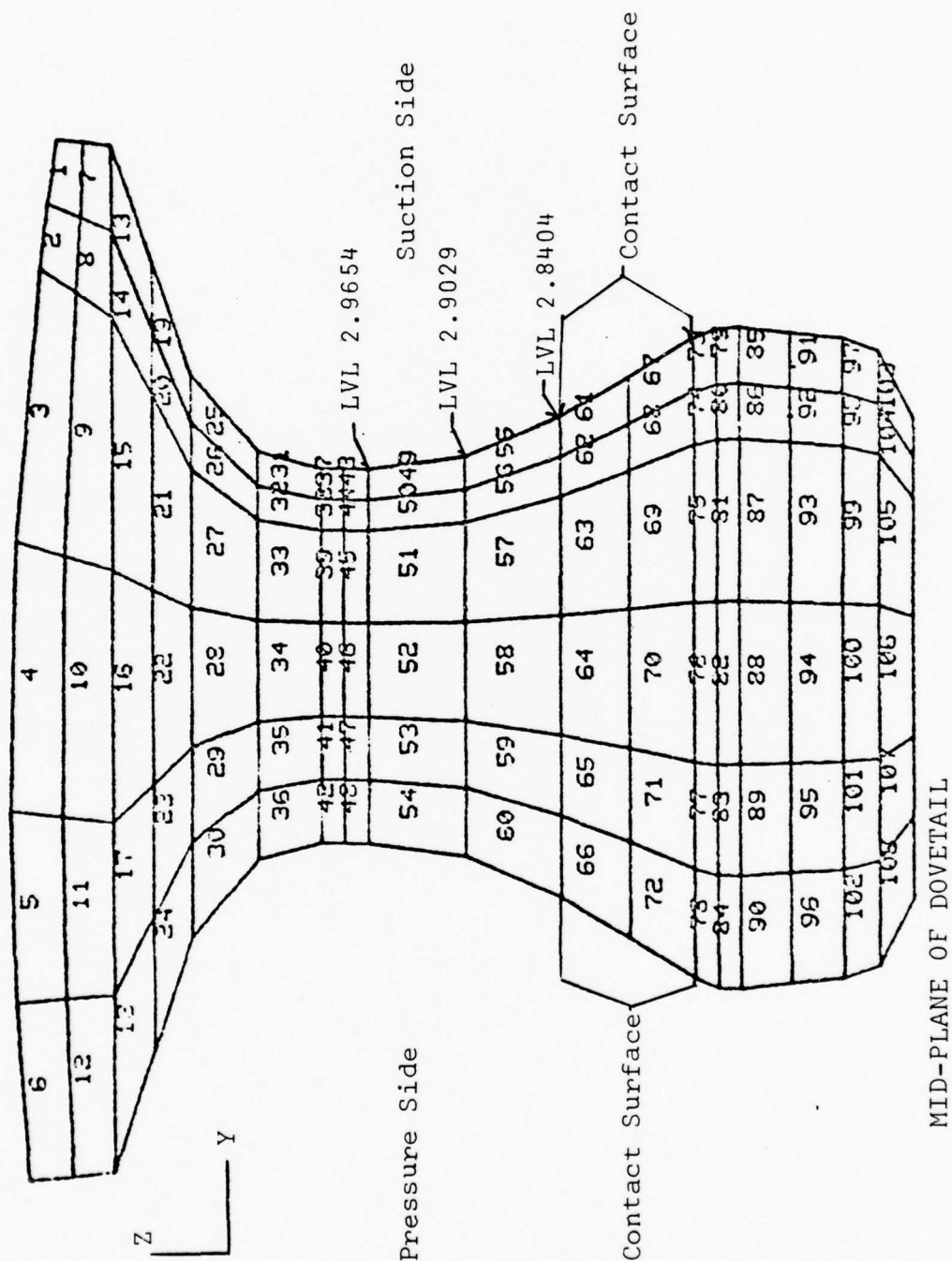
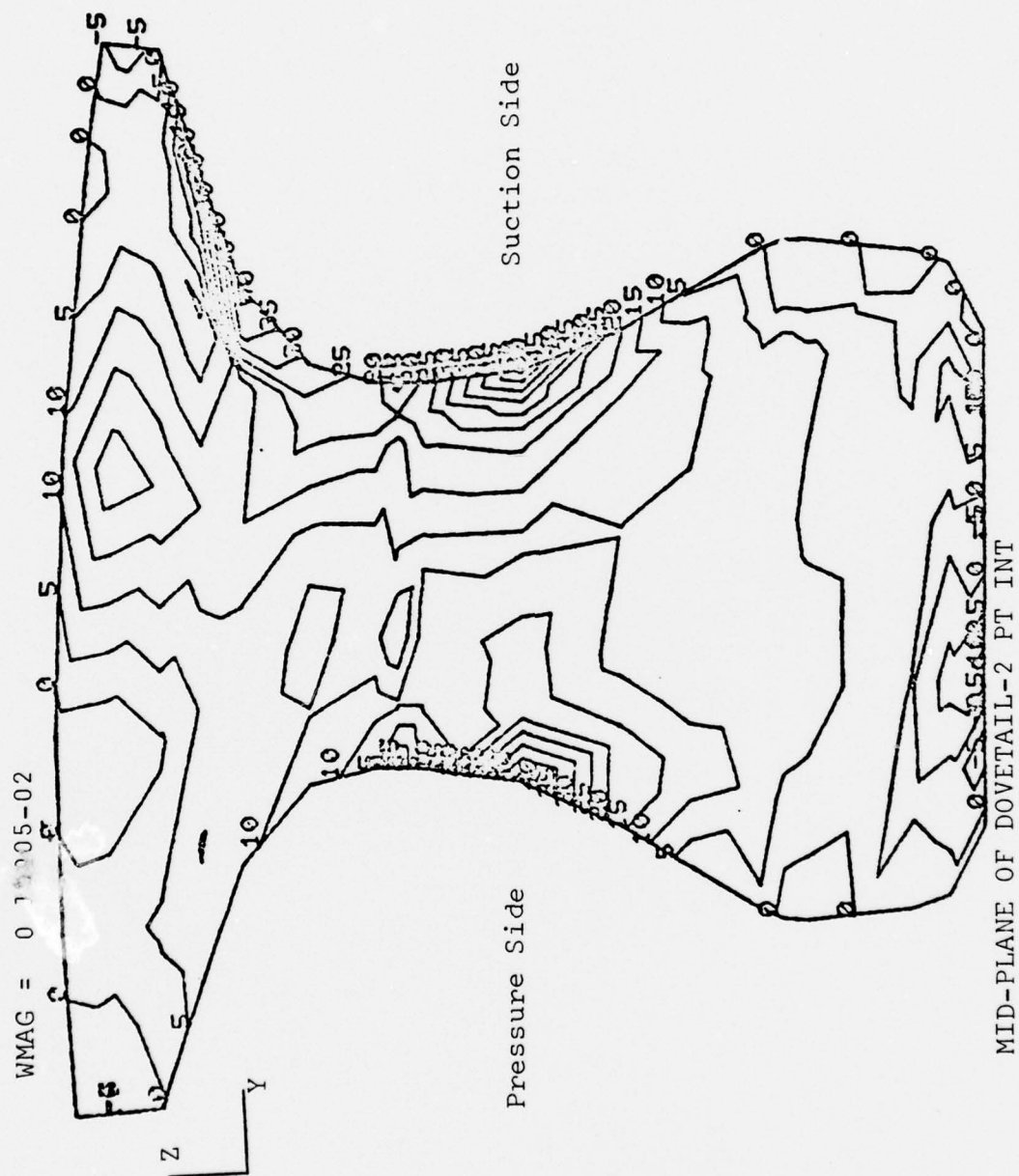


Figure 9. Attachment Root Finite Element Mesh.



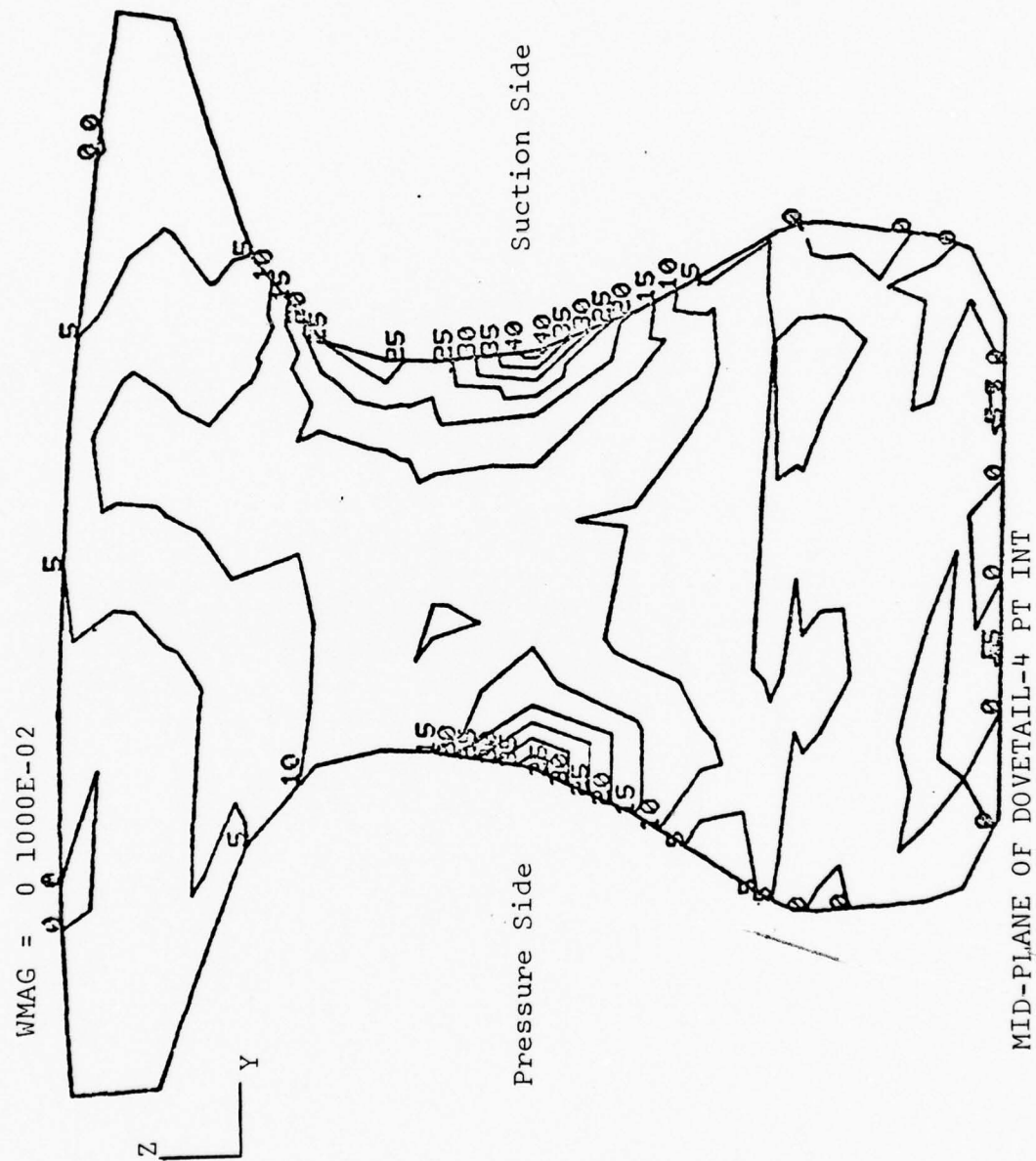
(a) 2-D Element Arrangement

Figure 10. Mid-Plane Dovetail Cross-Section,
Page 1 of 3.



(a) Maximum Principal Stress Isolines for 2-pt Order Integration (ksi)

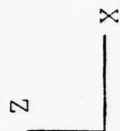
Figure 10. Continued, Page 2 of 3.



(b) Maximum Principal Stress Iso-
lines for 4-pt Order Integration (ksi)

Figure 10. Continued, Page 3 of 3.

A: Level 2.9654
 B: Level 2.9029
 C: Level 2.8404
 D: Contact Surface



	2	3	4	5	6
7	8	9	10	11	12
13	14	15	16	17	18
19	20	21	22	23	24
25	26	27	28	29	30
31	32	33	34	35	36
37	38	39	40	41	42
43	44	45	46	47	48
49	50	51	52	53	54
55	56	57	58	59	60
61	62	63	64	65	66
67	68	69	70	71	72
73	74	75	76	77	78
79	80	81	82	83	84
85	86	87	88	89	90
91	92	93	94	95	96
97	98	99	100	101	102
103	104	105	106	107	108

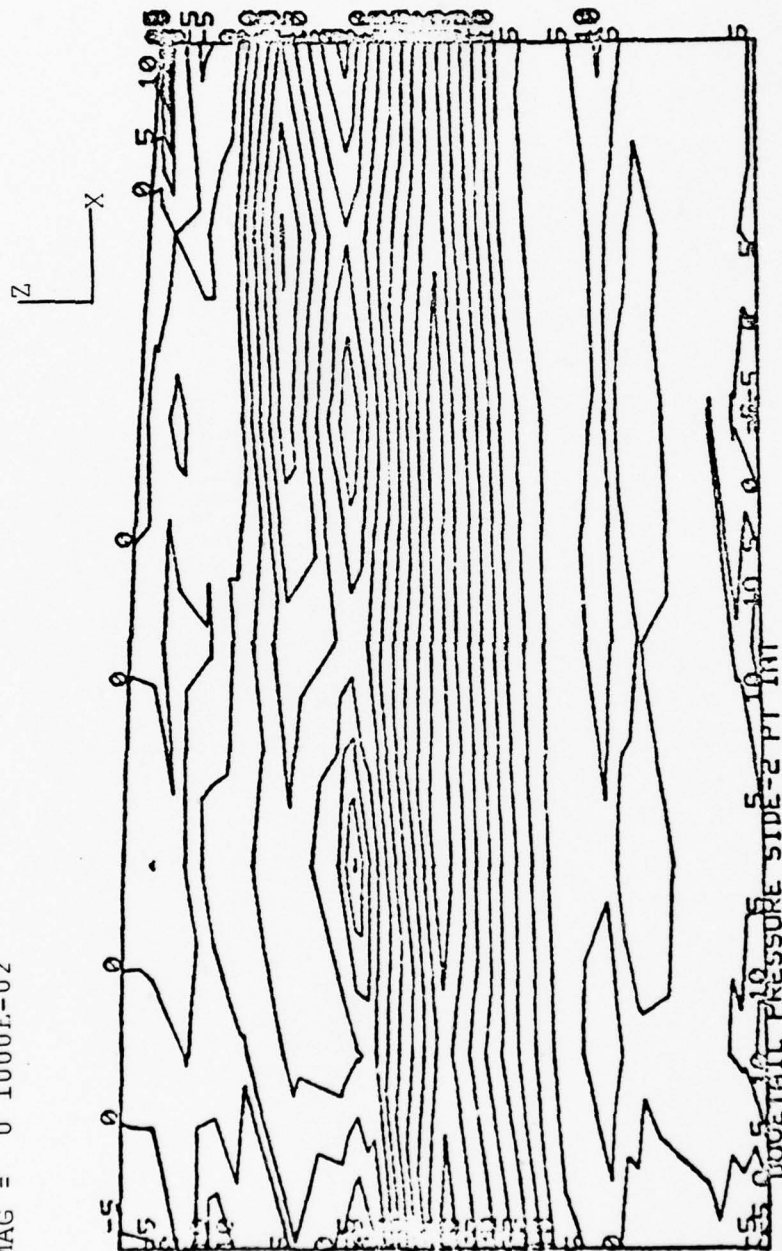
A D C D

DOVETAIL PRESSURE SIDE

(a) 2-D Element Arrangement

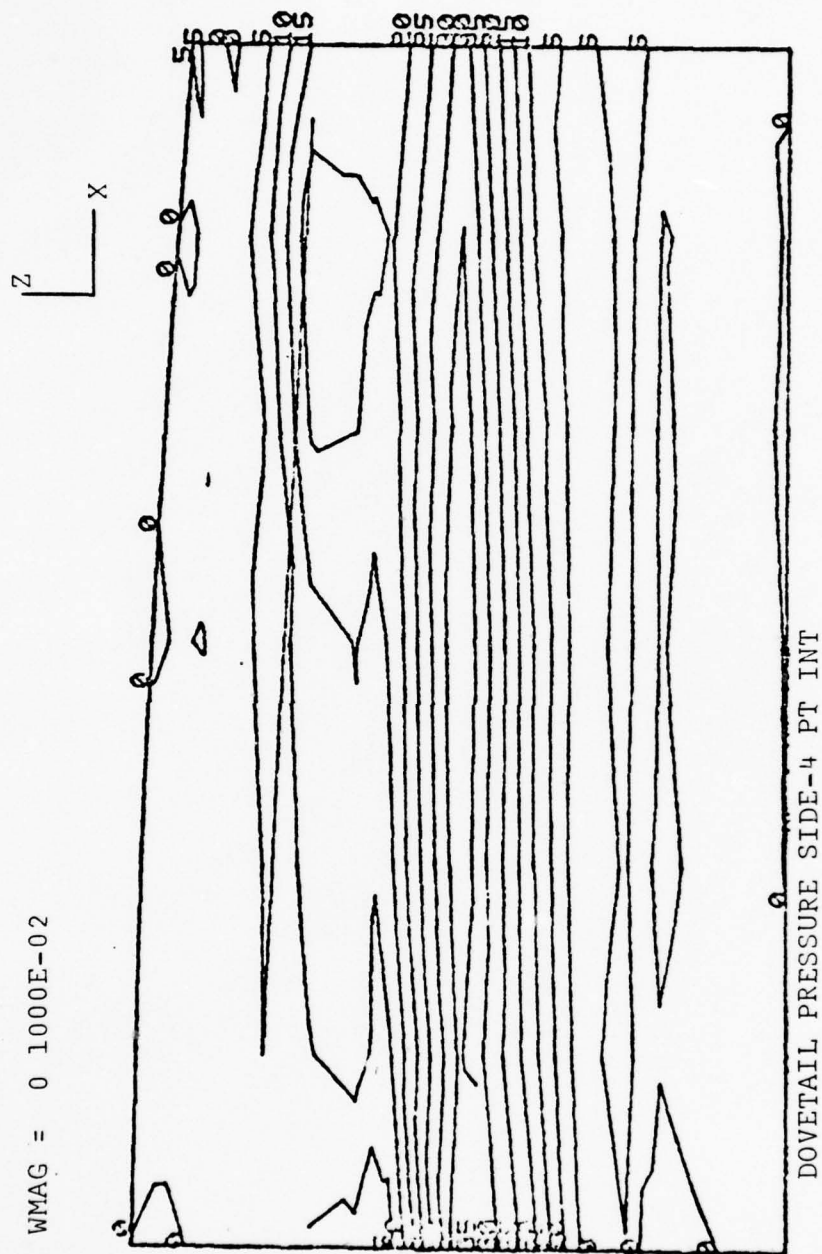
Figure 11. Dovetail Pressure Side,
 Page 1 of 3.

WMAG = 0 1000E-02



(b) Maximum Principal Stress Iso-lines
for 2-pt Order Integration (ksi)

Figure 11. Continued, Page 2 of 3.



(c) Maximum Principal Stress Iso-lines
for 4-pt Integration Order (ksi)

Figure 11. Continued, Page 3 of 3.

Z
X

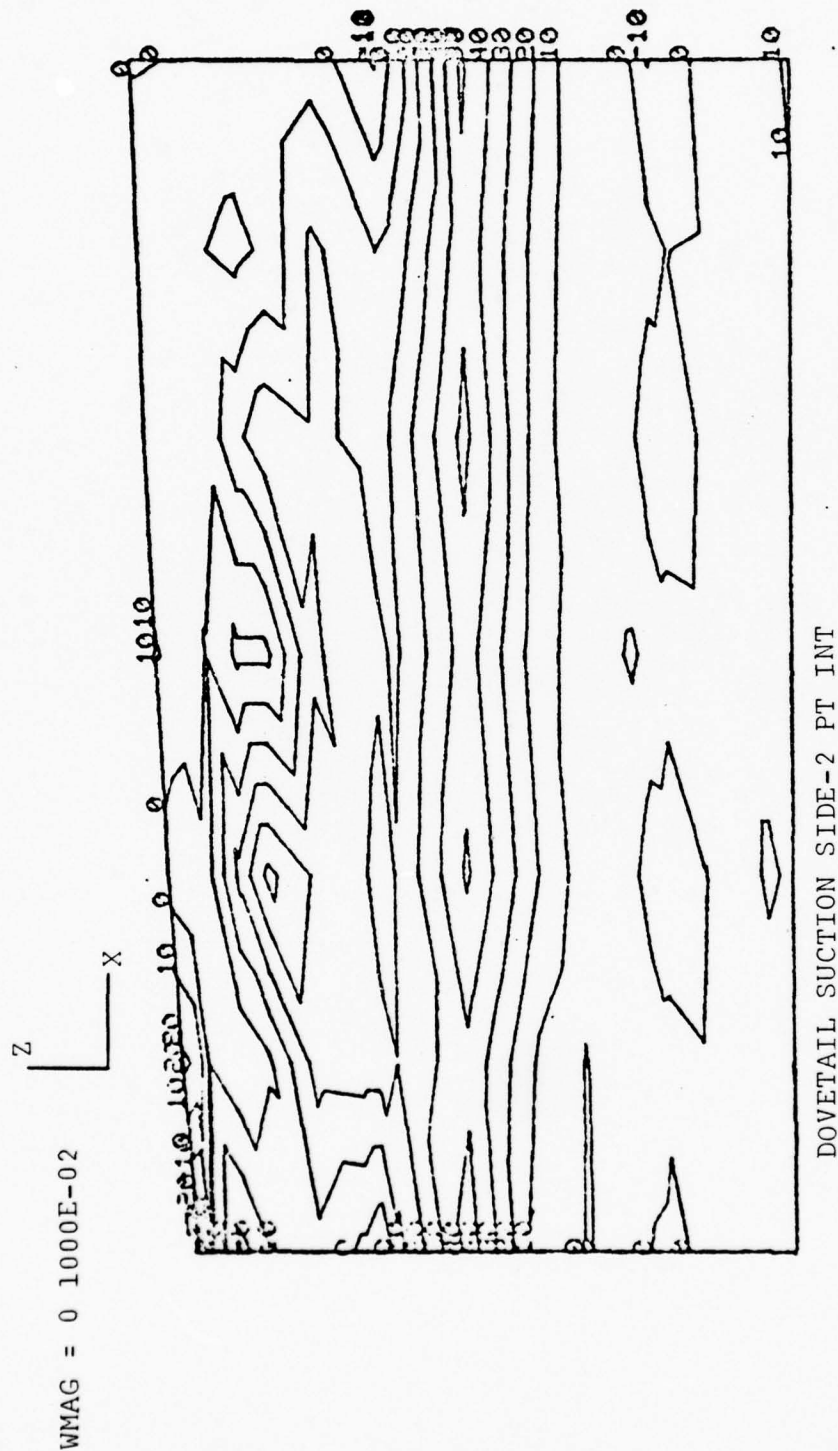
A: Level 2.9654
B: Level 2.9029
C: Level 2.8404
D: Contact Surface

	1	2	3	4	5	6
1	1	2	3	4	5	6
12	12	14	15	16	17	18
19	19	20	21	22	23	24
25	25	26	27	28	29	30
31	31	32	33	34	35	36
37	37	38	39	40	41	42
43	43	44	45	46	47	48
54	54	50	51	52	53	54
55	55	56	57	58	59	60
61	61	62	63	64	65	66
67	67	68	69	70	71	72
73	73	74	75	76	77	78
85	85	86	87	88	89	90
91	91	92	93	94	95	96
97	97	98	99	100	101	102
103	103	104	105	106	107	108

DOVETAIL SUCTION SIDE

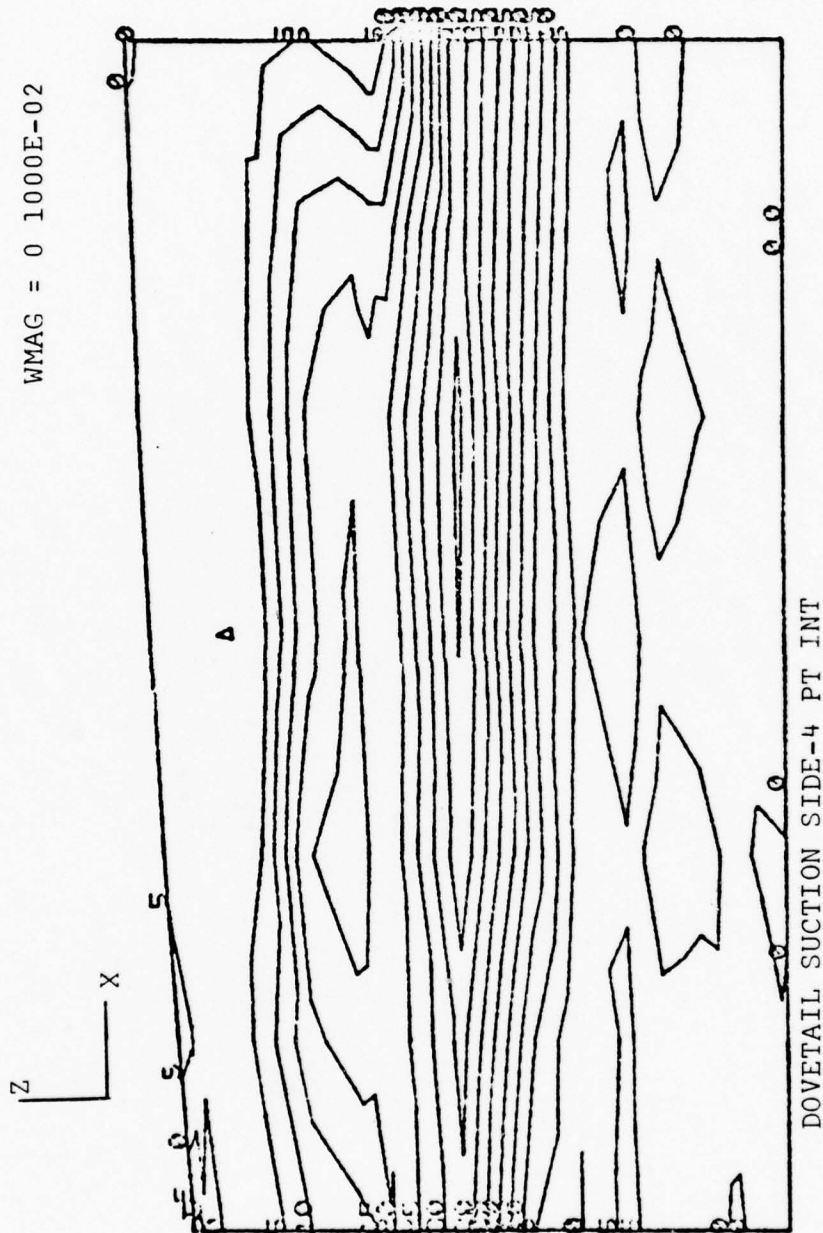
(a) 2-D Element Arrangement

Figure 12. Dovetail Suction Side,
Page 1 of 3.



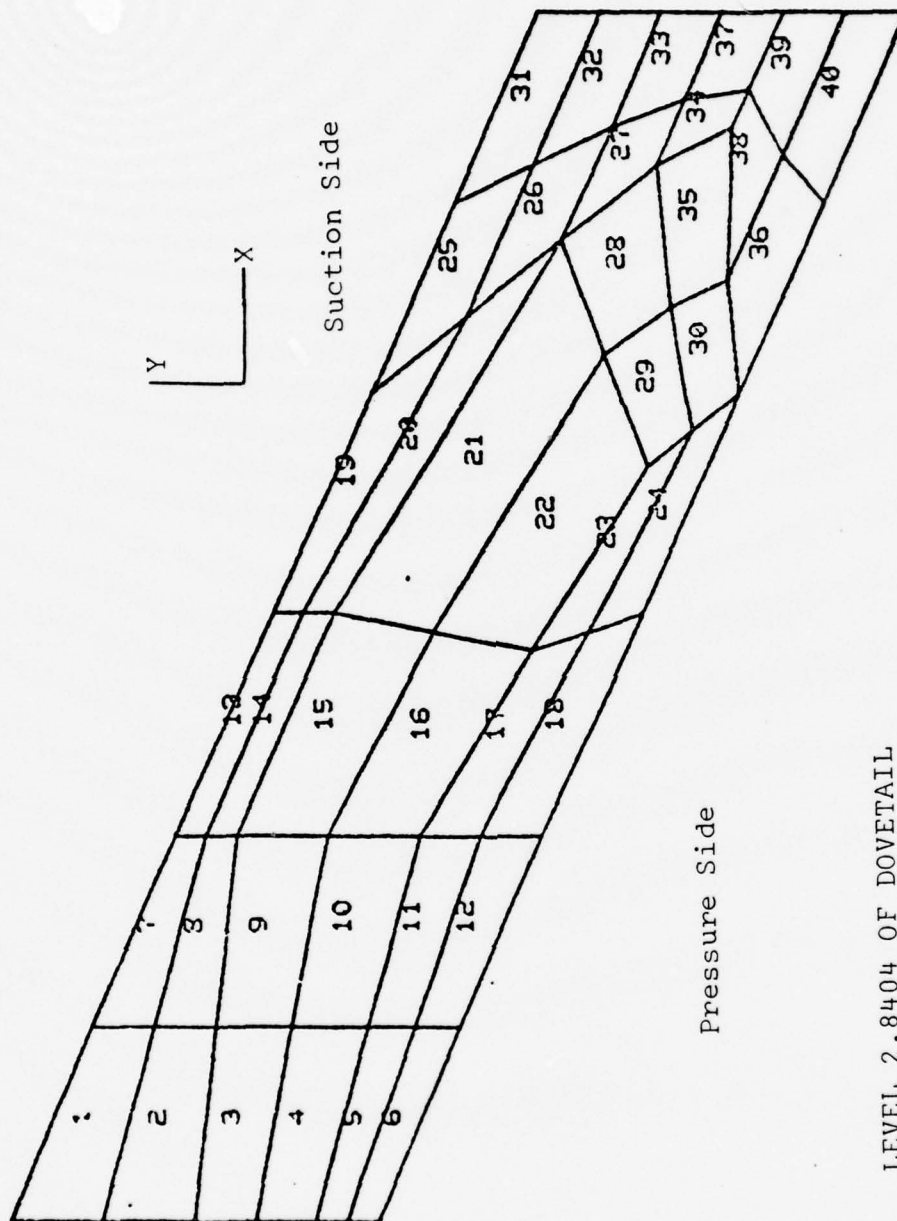
(b) Maximum Principal Stress Iso-lines
for 2-pt Integration Order (ksi)

Figure 12. Continued, Page 2 of 3.



(c) Maximum Principal Stress Iso-lines
for 4-pt Integration Order (ksi)

Figure 12. Continued, Page 3 of 3.

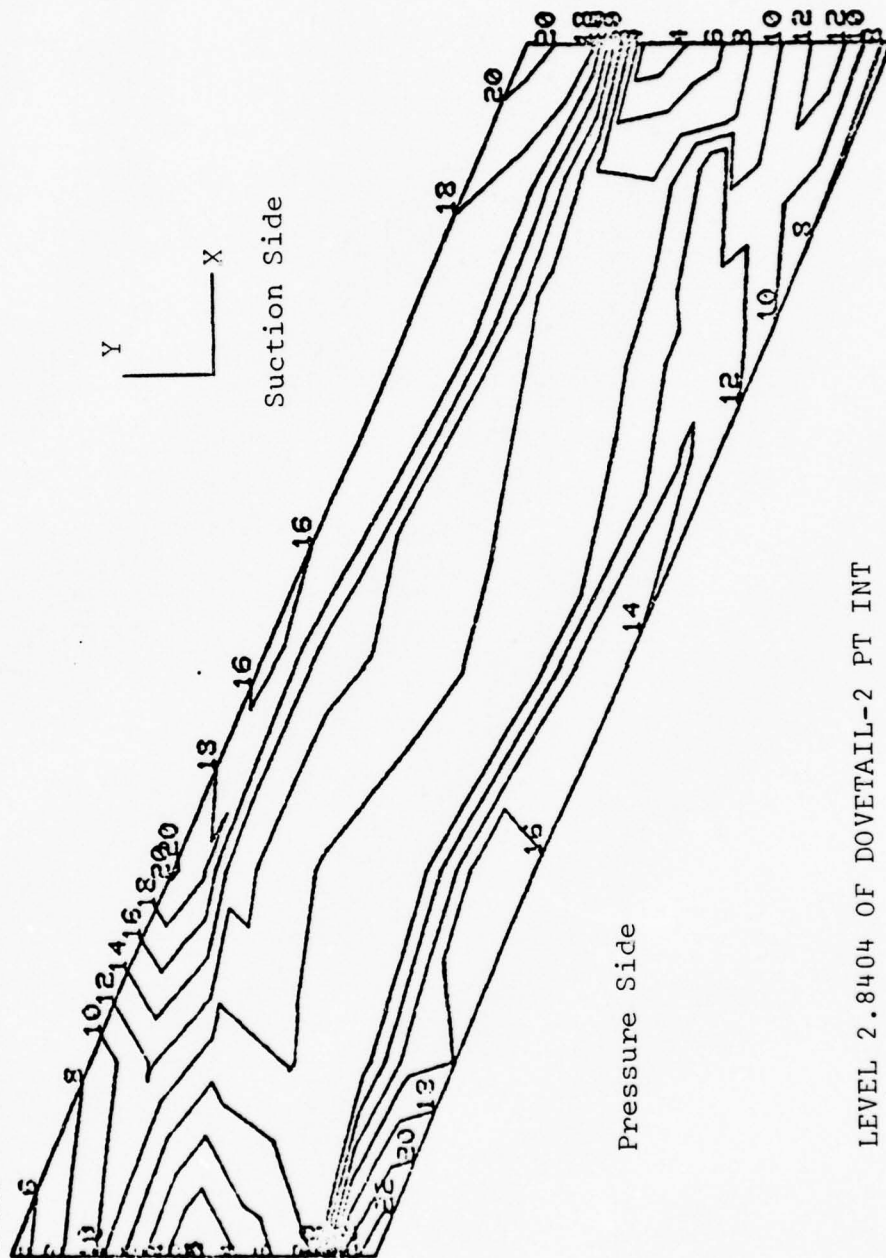


LEVEL 2.8404 OF DOVETAIL

(a) 2-D Element Arrangement

Figure 13. Level 2.8404, Page 1 of 3.

WMAG = 0 1000E-02

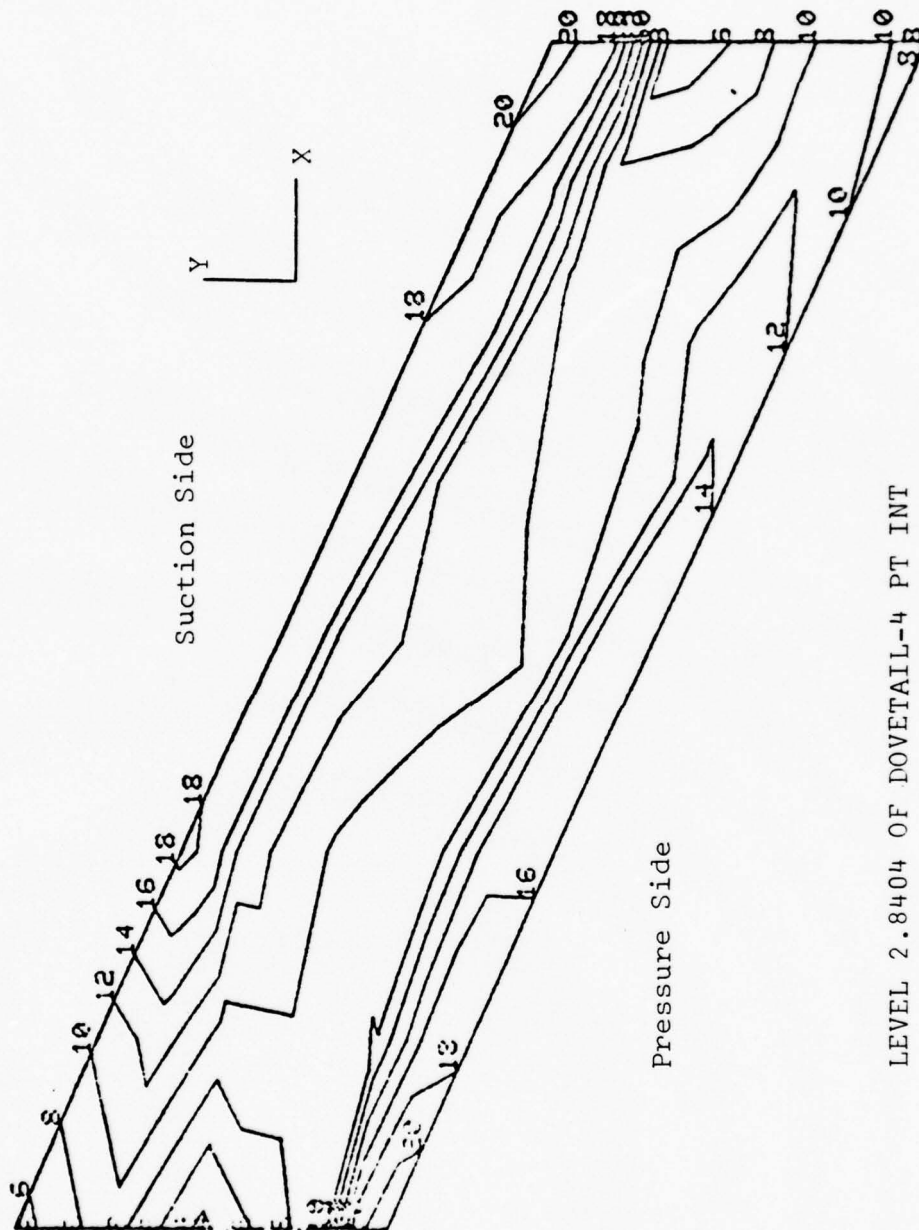


LEVEL 2.8404 OF DOVETAIL-2 PT INT

(b) Maximum Principal Stress Iso-lines
for 2-pt Integration Order (ksi)

Figure 13. Continued, Page 2 of 3.

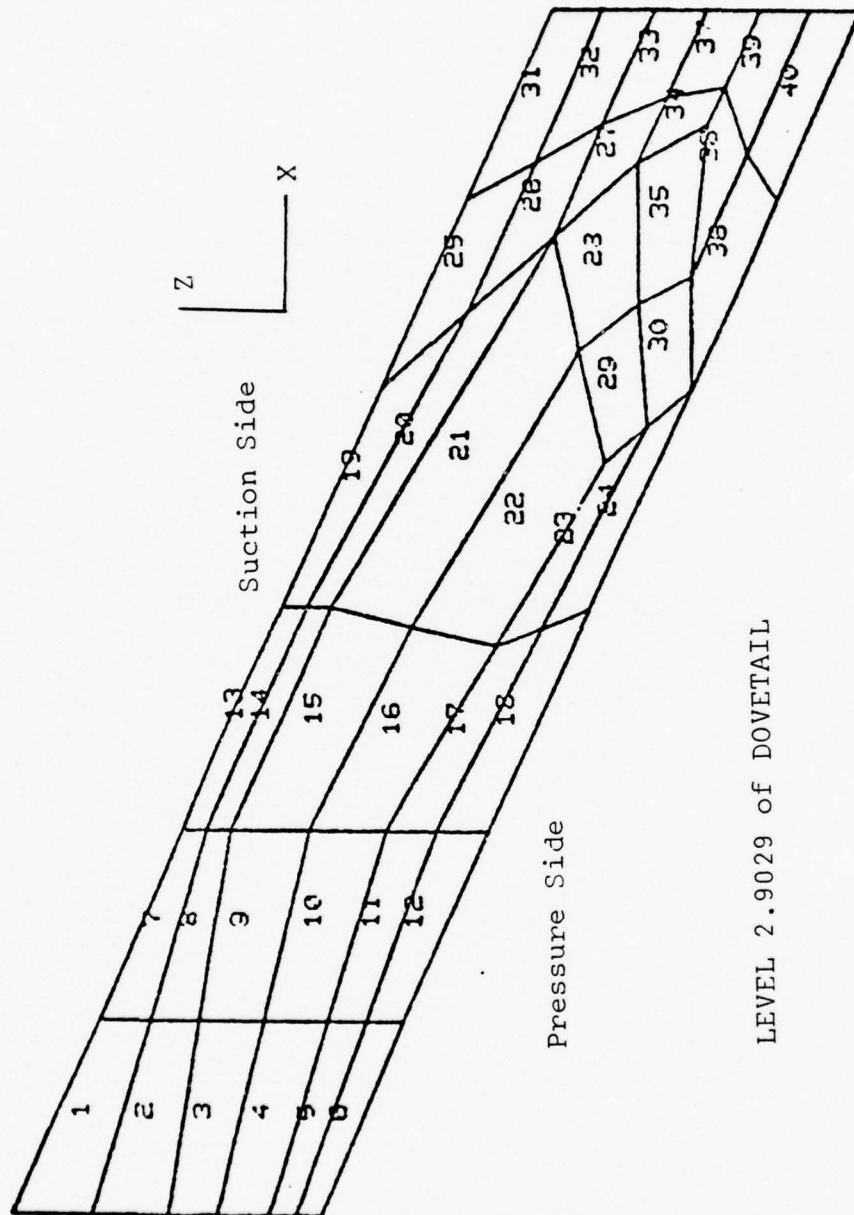
WMAG = 0 1000E-02



LEVEL 2.8404 OF DOVETAIL-4 PT INT

(c) Maximum Principal Stress Iso-lines
for 4-pt Integration Order (ksi)

Figure 13. Continued, Page 3 of 3.

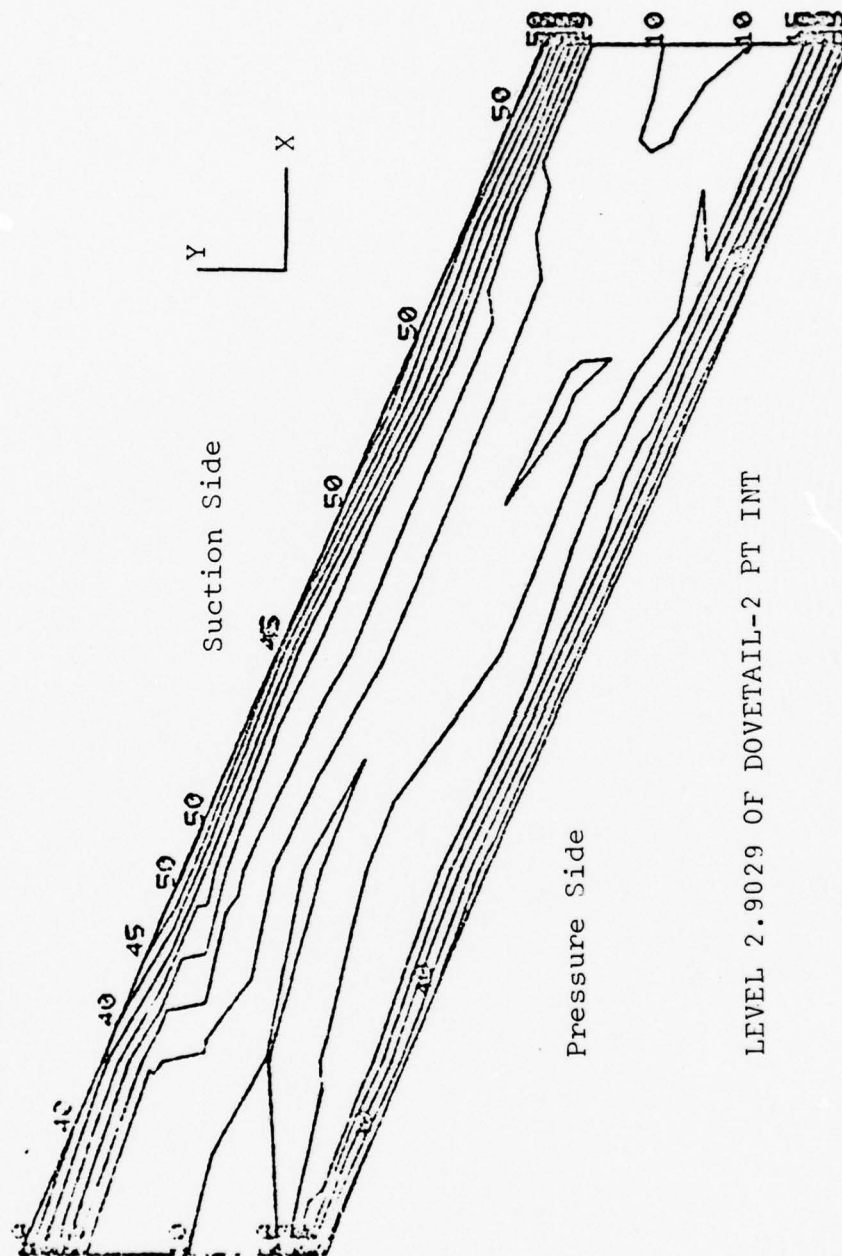


LEVEL 2.9029 of DOVETAIL

(a) 2-D Element Arrangement

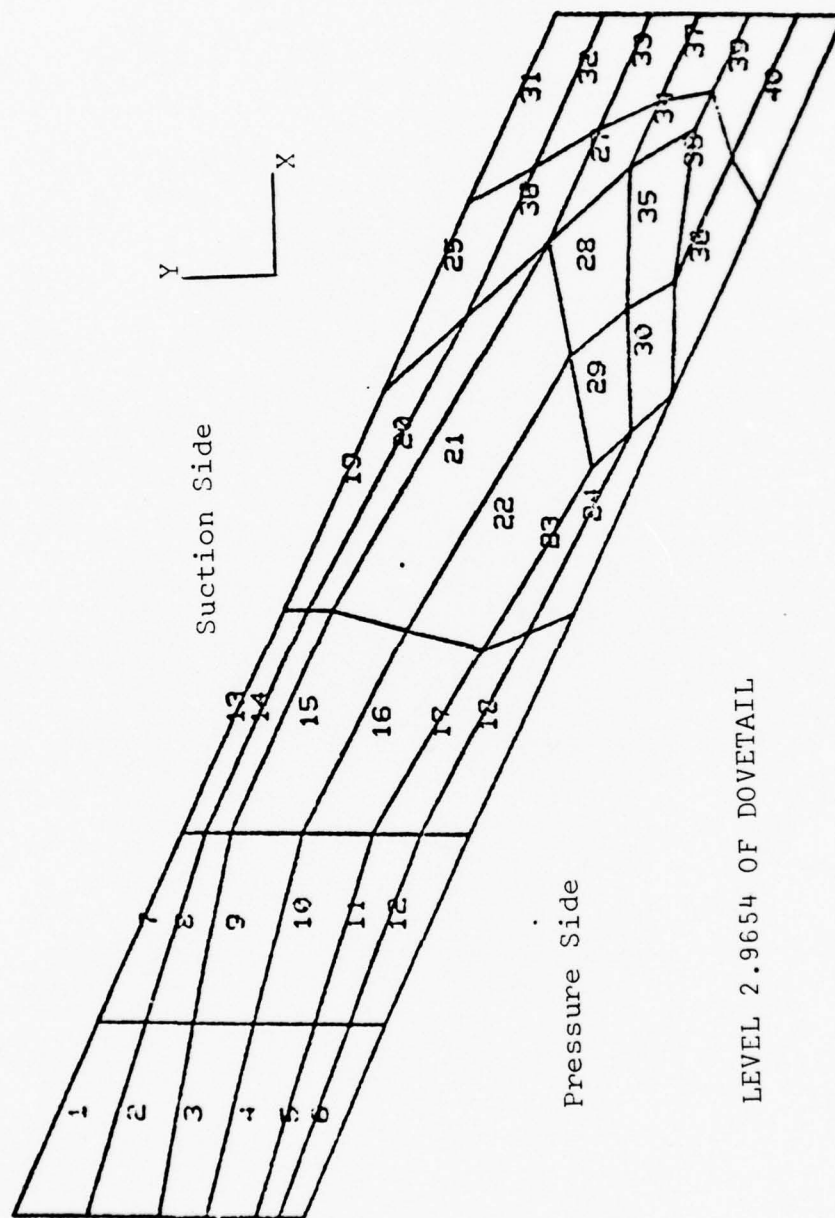
Figure 14. Level 2.9029, Page 1 of 3.

WMAG = 0 1000E-02



(b) Maximum Principal Stress Iso-lines
for 2-pt Integration Order (ksi)

Figure 14. Continued, Page 2 of 3.

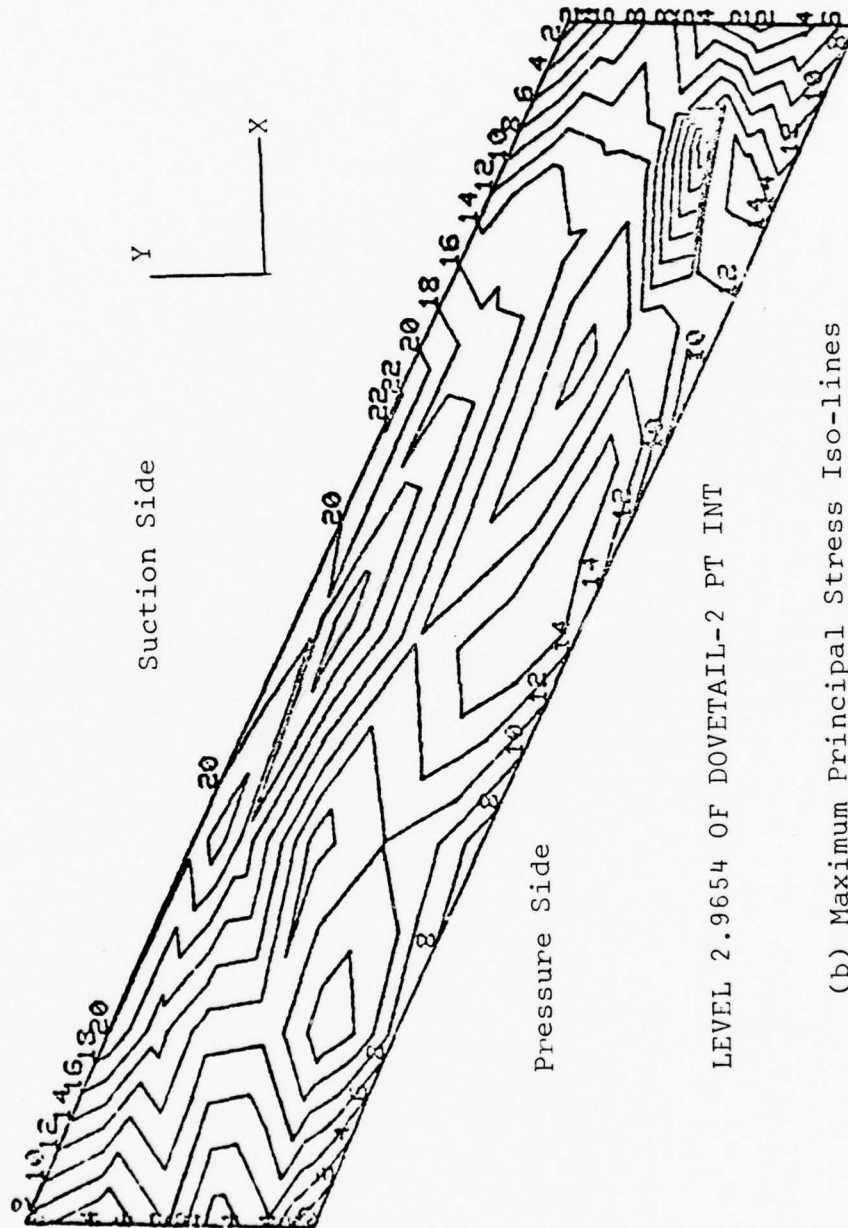


LEVEL 2.9654 OF DOVETAIL

(a) 2-D Element Arrangement

Figure 15. Level 2.9651, Page 1 of 3.

WMAG = 0 1000E-02



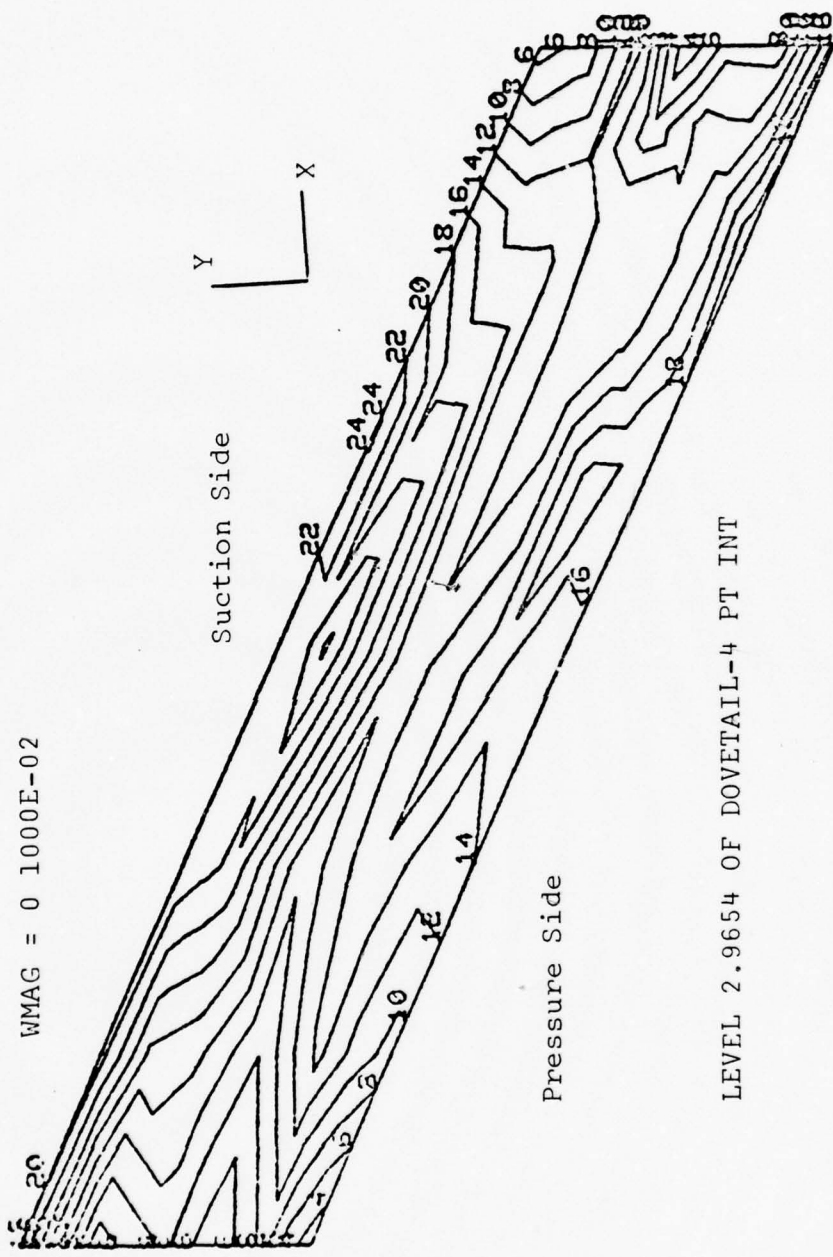
Pressure Side

Suction Side

LEVEL 2.9654 OF DOVETAIL-2 PT INT

(b) Maximum Principal Stress Iso-lines
for 2-pt Integration Order (ksi)

Figure 15. Continued, Page 2 of 3.



WMAG = 0 1000E-02

Suction Side

Pressure Side

LEVEL 2.9654 OF DOVETAIL-4 PT INT

(c) Maximum Principal Stress Iso-lines
for 4-pt Integration Order (ksi)

Figure 15. Continued, Page 3 of 3.

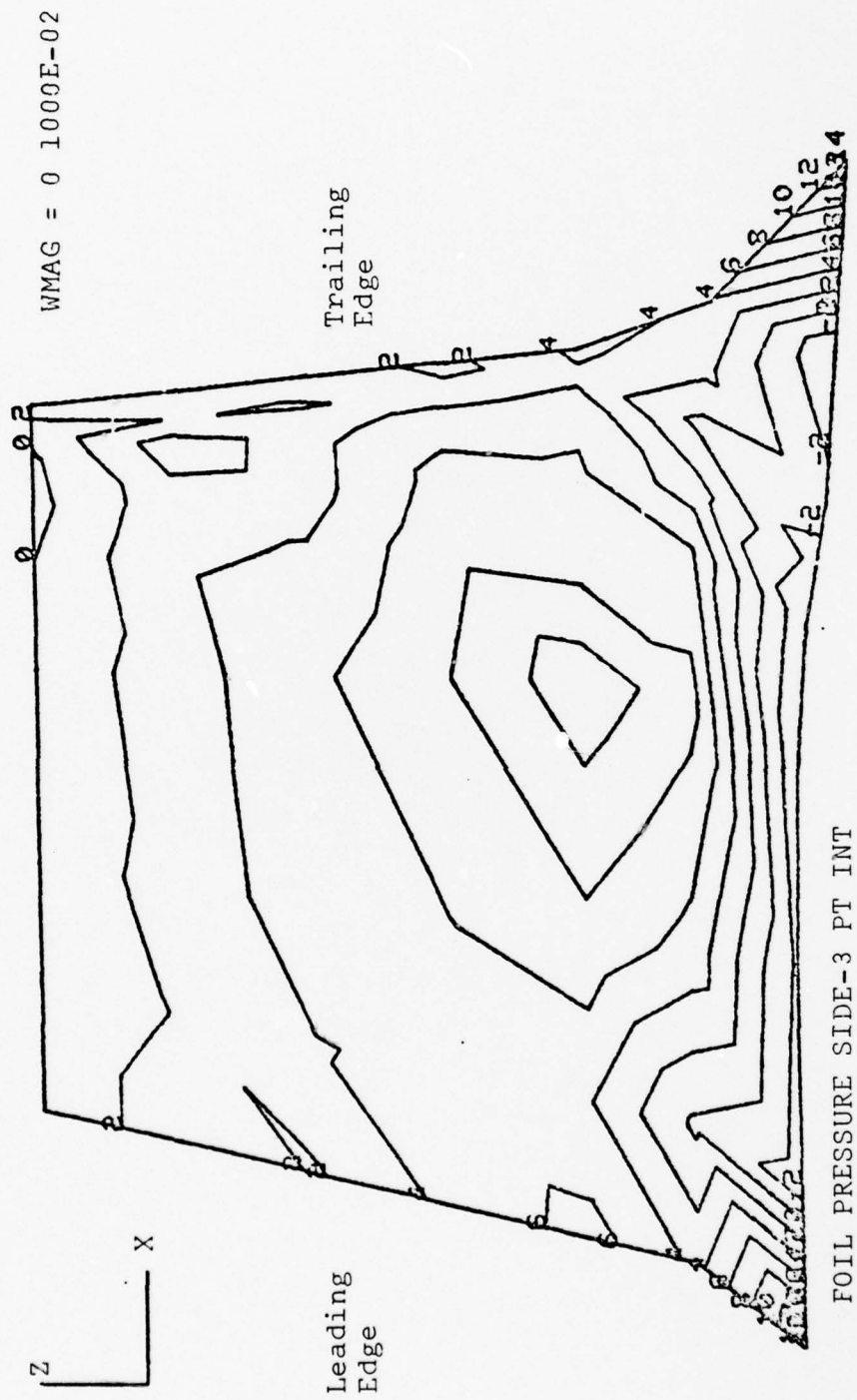


Figure 16. Maximum Principal Stress Contours for Pressure Side of Airfoil (ksi).

WMAG = 0 1000E-02

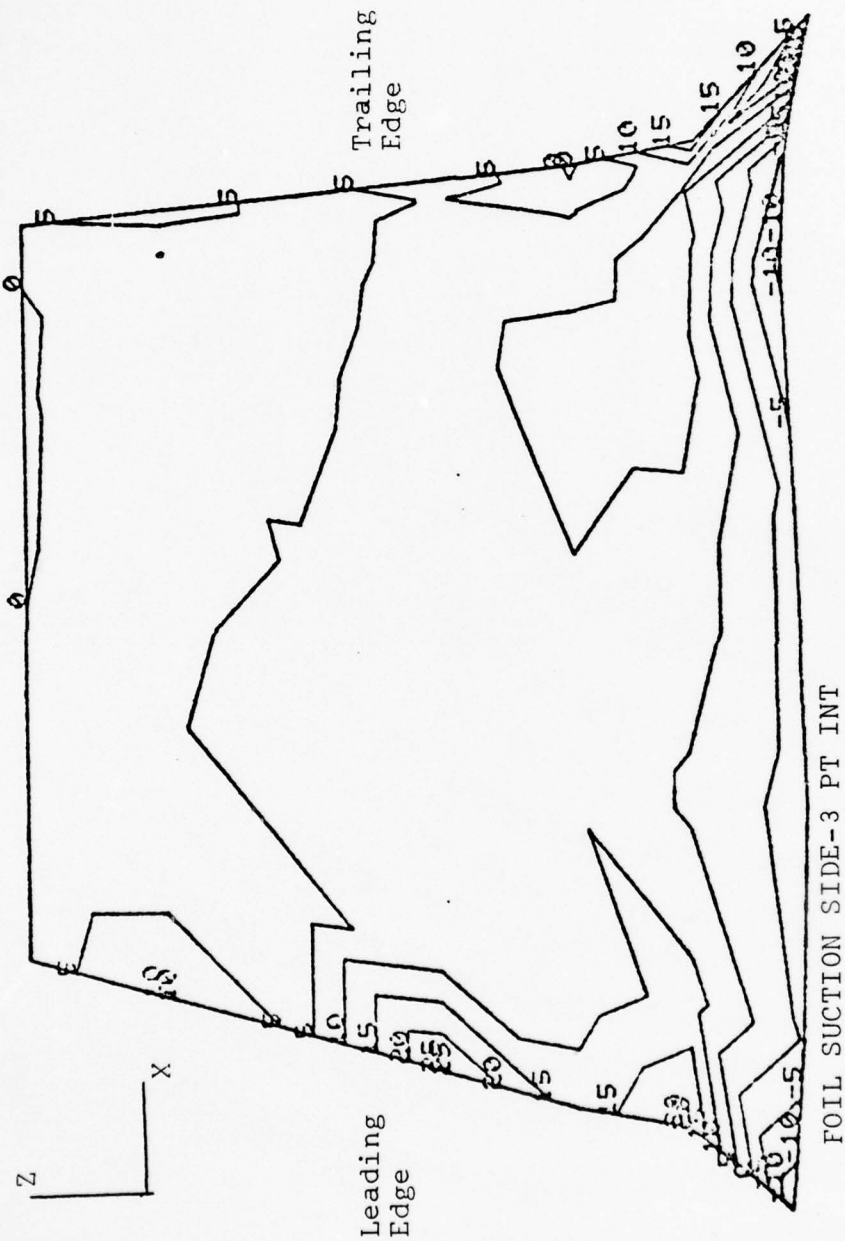


Figure 17. Maximum Principal Stress Contours for Suction Side of Airfoil (ksi).

VII. CONCLUSIONS

The time required for development of pre- and post-processors prevented a complete analysis which would have the potential for strong conclusive opinions and possible suggestions for design improvement. Software and hardware tools are, however, now implemented and identified which will allow follow-on analysis by NPS thesis students of geometric complex machine components. Despite the handicap of an inconclusive analysis, certain comments can be made concerning the results.

A. ANALYSIS RESULTS

Three other finite element analyses of ceramic turbine blade designs were reviewed by the author [Refs. 9, 10, 11]. Despite differing boundary conditions and loading schemes, a surface stress concentration persists in the region immediately above the blade-disk contact surface. This fact indicates that further research is required into the possibility of optimizing the dovetail geometry in order to spread the stresses over a greater bulk of material. If such an optimized design proves infeasible or non-existent, then the conclusion of this analysis and review indicates that hot-pressed Silicon-Nitride is unsuitable even for the limited goals of the current project. Using the four point bending strength of seventy-two ksi [Ref. 9] as a reference strength parameter, a simplistic factor of safety of 1.57 is realized. Considering the analysis did not impose

pressure and temperature gradient induced stresses, this factor of safety appears to be quite inadequate for predicting a decent probability of success.

Despite somewhat severe distortions in many of the analysis model elements, no mathematical singularities were encountered in using a reduced integration order. Further analysis using finer meshes may show that the reduced integration results are more accurate than the "exact" integration order. Should this be the case, approximately fifteen per cent higher values would be predicted than the results of "exact" integration of the stiffness matrix elements. These higher values would necessarily reduce the probability of success calculations normally used in design.

B. OPPORTUNITIES FOR FURTHER RESEARCH

The computer hardware and software at NPS, together with the groundwork laid by this thesis, allows for many avenues of follow-on research of which the following is a partial list:

- 1) refinement of the mesh of this analysis and convergence study of results,
- 2) analysis of the blade loaded under pressure and temperature gradient induced stresses,
- 3) optimization of attachment root design in order to alleviate stress concentrations,

- 4) probabilistic failure analysis using ADINA generated stresses,
- 5) frequency analysis of the blade,
- 6) investigation of appropriate boundary conditions,
- 7) analysis of the three material system of the blade-disk contact region.

APPENDIX A

ADDENDUM TO ADINA USER'S MANUAL, REPORT
82448-1, MIT, SEPTEMBER 1975
(Revised May 1976)

Two additional output options are available to the ADINA user at the Naval Postgraduate School besides what is described in the published user's manual. Master Control Card one, documented on page II.1, may be altered as follows:

NOTES	COLUMNS	VARIABLE	ENTRY
(a)	71-75	ITP57	Indicator for extended stress output and storage of stresses on user defined file 57. EQ.0; option not desired EQ.1; option desired
(b)	76-80	ITP58	Indicator for storage of displacements on user defined file 58. EQ.0; option not desired EQ.1; option desired

NOTES:

(a) The use of this option gives the user an output of stresses at all twenty-seven locations per element described in Section X.3 and illustrated on page X.37. Stresses are stored sequentially on user defined file 57 in the following order:

INPUT STEP

1. element number
2. integer 1 corresponding to figure X.5
3. normal stress for node in global X direction
4. normal stress for node in global Y direction
5. normal stress for node in global Z direction
6. shear stress XY
7. shear stress XZ
8. shear stress YZ

Steps 2 through 8 are repeated for the remainder of the twenty-seven nodes of the element, followed by a complete cycle for each of the remaining elements.

(b) Use of this option stores the six global displacements for each node on user defined file 58 in the following order:

INPUT STEP

1. node number
2. X direction displacement
3. Y direction displacement
4. Z direction displacement
5. X-axis rotation (if present)
6. Y-axis rotation (if present)
7. Z-axis rotation (if present)

Steps 1 through 7 are repeated for each of the input nodes. Displacements for the additional nodes for which stress results are calculated with option ITP57 are not calculated.

APPENDIX B

CONVERSION OF CALCOMP PLOTTING ROUTINES FOR USE ON A TEKTRONIX 4012 TERMINAL

The TEKTRONIX 4012 Computer Display Terminal is the most powerful interactive graphics system available to the general user at the Naval Postgraduate School. The major advantages of this unit are its speed and access to the IBM 360 computer via the CP/CMS system. A major disadvantage is there is only one terminal designated for the general user. During the final stages of preparation of this report, PSAP1 and Program Contour Plot were modified for use with the TEKTRONIX terminal in order to achieve a higher quality of plot in a timely manner than is possible with the CALCOMP system. These modifications proved quite simple and resulted in a usable plotting system. Presented in this appendix are the subroutines added to the graphics programs used by the author and a few general comments. The user should consult Refs. 12, 13, 14 and 15 for detailed information on using the TEKTRONIX unit.

The user must first determine the plotting origin of his routine and establish the limits of his plotting window using subroutine VWINDO. Caution must be used in order to ensure that the original program will properly scale the plotting values in both coordinate directions. CALCOMP PLOT statements which shift the origin must be deleted. Subroutines must then be added to the routine which are titled with CALCOMP plotting library routine names which in turn

call equivalent subroutines in the TEKTRONIX library. The following are examples used with PSAP1 and Program Contour Plot:

1) Subroutine equivalent to CALCOMP PLOTS:

```
SUBROUTINE PLOTS
  IBAUD=480
  CALL INITT (IBAUD)
  CALL BINITT
  RETURN
END
```

2) Subroutine equivalent to CALCOMP PLOTE:

```
SUBROUTINE PLOTE
  IX=0
  IY=780
  CALL FINITT (IX,IY)
  RETURN
END
```

3) Subroutine equivalent to CALCOMP LINE:

```
SUBROUTINE LINE (Y,X,N,N1,N2)
  DIMENSION X(21), Y(21)
  CALL MOVEA (X(1),Y(1))
  DO 10 I=2,N
  CALL DRAWA (X(I),Y(I))
10 CONTINUE
  RETURN
END
```

4) Subroutine equivalent to CALCOMP NUMBER:

```
SUBROUTINE NUMBER (Y,X,H,AL,TH,N)
  DIMENSION IARRAY (4)
  CALL MOVEA (X,Y)
  CALL IFORM (AL,4,IARRAY,32)
  DO 10 I=1,4
  IF (IARRAY(I).EQ.32) GO TO 10
  CALL ANCHO (IARRAY(I))
10 CONTINUE
  RETURN
END
```

5) Subroutine equivalent to CALCOMP SYMBOL:

```
SUBROUTINE SYMBOL (IY,IX,H,BCK,TH,N)
DIMENSION IARRAY (80), BCK (1)
CALL CONETA (BCK,N,IARRAY)
CALL NOTATE (IX,IY,N,IARRAY)
RETURN
END
```

6) Subroutine equivalent to CALCOMP PLOT:

```
SUBROUTINE PLOT (Y,X,I)
IF (I.EQ.2) CALL DRAWA (X,Y)
IF (I.EQ.3) CALL MOVEA (X,Y)
RETURN
END
```

These subroutines were tailored for use only with PSAP1 and Program Contour Plot and are much more restrictive than the CALCOMP equivalent. For example, subroutine NUMBER defined above will only plot integers up to four digits whereas subroutine NUMBER used with the CALCOMP will plot any integer or floating point number input by the user. The subroutines do, however, provide an example of the simple modifications required and the TEKTRONIX software is available for a much higher degree of graphics sophistication.

NOT
Preceding Page BLANK - FILMED

(This page intentionally blank)

PROGRAM CENTRIFUGAL LOAD LISTING

```

PROGRAM CENTRIFUGAL LOAD
THIS PROGRAM READS AN ADINA INPUT DECK AND CALCULATES NODAL
CONSTANT LOADS CAUSED BY A GIVEN ROTATION ABOUT ANY COMBI-
NATION OF RIGHT-HAND CARTESIAN COORDINATE SYSTEM AXES.
VARIOUS CHOICES OF OUTPUTS CAN BE SELECTED INCLUDING A
PUNCHED CARD DECK IN A FORMAT ACCEPTABLE TO ADINA FINITE
ELEMENT CODE FOR INPUT OF CONCENTRATED NCDAL FORCES.

INPUT DATA DECK
CARD 1 (FORMAT 4F10.0)
VARIABLE COL
W1 1-10
W2 11-20
W3 21-30
RO 31-40
REMARKS
ANGULAR VELOCITY ABOUT THE X-AXIS
ANGULAR VELOCITY ABOUT THE Y-AXIS
ANGULAR VELOCITY ABOUT THE Z-AXIS
MASS DENSITY

CARD 2 (FORMAT 8I5)
NUMNF 1-5
NUMEL 6-10
NGP 11-15
NCUR 16-20
ICLK1 21 25
ICLK2 26-30
ICLK3 31-35
NUMBER OF GAUSS POINT INTEGRATION (2-6)
ORDER OF CURVE NUMBER TO BE USED IN ADINA
LOAD SECTION XII OF ADINA USERS MANUAL
FLAG FOR PRINTOUT OF NODE COORDINATE AND
MESH CONNECTIVITY DATA
J-NO PRINTOUT
J-PRIN PRINTOUT
FLAG FOR PRINTOUT OF CONSISTANT LOADS
BY ELEMENT
J-NG PRINTOUT
J-PRIN PRINTOUT
FLAG FOR PRINTOUT CF TOTALED CONSISTANT
LOADS FOR EACH NOCE
J-NO PRINTOUT

```

[illegible]


```

1001 READ(5,1001)NUMNP,NUMEL,NGP,NCUR,ICHK1,ICHK2,ICHK3,ICHK4
      FCFORMAT(815)W1,W2,W3,RO
      WRITE(6,1002)NUMNP,NUMEL,NGP
1002 FCFORMAT(//5X,'ANGULAR VELOCITIES',/10X,'WX = ',G25.16/10X,'WY = ',
      1 G25.16/10X,'WZ = ',G25.16//5X,'DENSITY = ',G25.16//
1003 2 FCFORMAT(//5X,'NUMBER OF NODE POINTS = ',15//5X,'NUMBER OF
      3 ELEMENT = ',15//5X,'NUMBER OF GAUSS POINTS FOR INTERGRATION
      = ',15//)
      N1=1
      N2=N1+60*NUMEL
      N3=N2+NUMNP
      N4=N3+NUMNP
      N5=N4+NUMNP
      N6=N5+NUMNP
      N7=N6+NUMEL
      N8=N7+20*NUMEL
      NLAST=N8+3*NUMNP
      IF(NLAST.GT.MTOT)WRITE(6,2000)NLA
2000 1 FCFORMAT(//5X,'MTOT = ',15,' INCREASE MTCT FOR ADDITIONAL STORAGE
      1,//)
      CALL CENTF(A(N1),A(N2),A(N3),A(N4),A(N5),A(N6),A(N7),A(N8))
      STOP
      END
      SUBROUTINE CENTF(TFVT,XPT,YPT,ZPT,NUMPT,NREL,ACCNT,FORCE)
      *****
      SUBROUTINE TO COORDINATE INPUT AND OUTPUT CF
      CONSISTANT CENTRIFUGAL LOADS.
      *****
      IMPLICIT REAL*8 (A-H,O-Z)
      COMMON/PPARA/W1,W2,W3,RO
      COMMON/PPARA/NUMNP,NUMEL,NGP,NCUR,NPTM,IDGRAV
      COMMON/LOADS/NLOAD,NLCUR,NCHK2,ICHK3,ICHK4
      COMMON/CHECK/ICHK1,ICHK2,ICHK3,ICHK4
      DIMENSION XPT(1),YPT(1),ZPT(1),NUMPT(1),NREL(1)
      DIMENSION TFVT(20,3,1),FORCE(3,1),NCONT(20,1)
      CALL READIN(XPT,YPT,ZPT,NCONT,NREL,NUMPT)
      IF(ICHK1.EQ.0)GO TO 10
      CALL PNTOUT(XPT,YPT,ZPT,NCONT,NREL,NUMPT,FORCE)
      CALL TRANS(TFVT,XPT,YPT,ZPT,NCONT,NREL,NUMPT,FORCE)
      RETURN
      END
      SUBROUTINE TRANS (TFVT,XPT,YPT,ZPT,NCONT,NREL,NUMPT,FORCE)

```


300
 33310
 33320
 33330
 33340
 33350
 33360
 33370
 33380
 33390
 33400
 33410
 33420
 33430
 33440
 33450
 33460
 33470
 33480
 33490
 33500
 33510
 33520
 33530
 33540
 33550
 33560
 33570
 33580
 33590
 33600
 33610
 33620
 33630
 33640
 33650
 33660
 33670
 33680
 33690
 33700
 33710
 33720
 33730
 33740
 33750
 33760
 33770

```

    ENI(19) = GM(R)*GM(S)*GZ(T)
    IF(NCON(19).EQ.0) ENI(19) = ZRO
    IF(NCON(20).EQ.0) ENI(20) = ZRO
    ENI(1) = GM(R)*GM(S)*GP(T)
    ENI(2) = GM(R)*GM(S)*GP(T)
    ENI(3) = GM(R)*GM(S)*GP(T)
    ENI(4) = GM(R)*GM(S)*GP(T)
    ENI(5) = GM(R)*GM(S)*GP(T)
    ENI(6) = GM(R)*GM(S)*GP(T)
    ENI(7) = GM(R)*GM(S)*GP(T)
    ENI(8) = GM(R)*GM(S)*GP(T)
    IF(NCON(9).EQ.0) GO TO 500
    DNI(1,9) = DZ(R)*GP(S)*GP(T)
    DNI(2,9) = GZ(R)*GP(S)*GP(T)
    DNI(3,9) = GZ(R)*GP(S)*GP(T)
    IF(NCON(10).EQ.0) GO TO 510
    DNI(1,10) = DM(R)*GZ(S)*GP(T)
    DNI(2,10) = GM(R)*DZ(S)*GP(T)
    DNI(3,10) = GM(R)*GZ(S)*GP(T)
    IF(NCON(11).EQ.0) GO TO 520
    DNI(1,11) = DZ(R)*GM(S)*GP(T)
    DNI(2,11) = GZ(R)*DM(S)*GP(T)
    DNI(3,11) = GZ(R)*GM(S)*GP(T)
    IF(NCON(12).EQ.0) GO TO 530
    DNI(1,12) = DP(R)*GZ(S)*GP(T)
    DNI(2,12) = GP(R)*DZ(S)*GP(T)
    DNI(3,12) = GP(R)*GZ(S)*GP(T)
    IF(NCON(13).EQ.0) GO TO 540
    DNI(1,13) = DZ(R)*GP(S)*GM(T)
    DNI(2,13) = GZ(R)*DP(S)*GM(T)
    DNI(3,13) = GZ(R)*GP(S)*GM(T)
    IF(NCON(14).EQ.0) GO TO 550
    DNI(1,14) = DM(R)*GZ(S)*GM(T)
    DNI(2,14) = GM(R)*DZ(S)*GM(T)
    DNI(3,14) = GM(R)*GZ(S)*GM(T)
    IF(NCON(15).EQ.0) GO TO 560
    DNI(1,15) = DZ(R)*GM(S)*GM(T)
    DNI(2,15) = GZ(R)*DM(S)*GM(T)
    DNI(3,15) = GZ(R)*GM(S)*GM(T)
    IF(NCON(16).EQ.0) GO TO 570
    DNI(1,16) = DP(R)*GZ(S)*GM(T)
    DNI(2,16) = GP(R)*DZ(S)*GM(T)
    DNI(3,16) = GP(R)*GZ(S)*GM(T)
    IF(NCON(17).EQ.0) GO TO 580
    DNI(1,17) = DP(R)*GP(S)*GZ(T)
    DNI(2,17) = GP(R)*GP(S)*GZ(T)
    DNI(3,17) = GP(R)*GP(S)*GZ(T)
  
```

+ + + + +
 EMI(12)
 EMI(10)
 EMI(11)
 EMI(12)
 EMI(16)
 EMI(14)
 EMI(15)
 EMI(16)
 I(17))//TWO
 I(18))//TWO
 I(19))//TWO
 I(20))//TWO
 I(17))//TWO
 I(18))//TWO
 I(19))//TWO
 I(20))//TWO

500
 510
 520
 530
 540
 550
 560
 570

[illegible]


```

700 DTJ = A1+A2+A3 - (B1+B2+B3)
   IF(DTJ.LE.ZERO) GO TO 960
   A(1,1) = W2*W2 + W3*W3
   A(2,2) = W3*W3 + W1*W1
   A(3,3) = W1*W1 + W2*W2
   A(1,2) = -W1*W2
   A(1,3) = -W1*W3
   A(2,3) = -W2*W3
   A(2,1) = A(1,2)
   A(3,1) = A(1,3)
   A(3,2) = A(2,3)
   DC 700 I=1,3
   PRODI(I)=0.000
   DC 700 J=1,20
   PRODI(I)=PRODI(I)+EMI(J)*COD(J,I)
700 DC 800 I=1,3
   PRODI(I)=0.000
   DC 800 J=1,3
   PRODI(I)=PRODI(I)+A(I,J)*PRODI(J)
800 DC 900 I=1,20
   FVT(I,J)=EMI(I)*PRODI(J)
900 DC 950 I=1,20
   FVT(I,J) = FVT(I,J)*DTJ
950 RETURN
560 WRITE(6,1000) IEL,DTJ,R,S,T
1000 FORMAT(//,5X,'ELEMENT NUMBER ',I5,' HAS A JACOBIAN DETERMINANT',/
1,5X,'OF VALUE ',1625.16,' *** EXECUTION STOPS ***./,
2,5X,' R = ',G25.16/5X,' S = ',G25.16/5X,' T = ',G25.16//)
   STOP
   END
SLROUTINE PNTOUT(XPT,YPT,ZPT,NCGT,NREL,NUMPT)
*****
SUBROUTINE TO PRINT OUT NODE AND ELEMENT INFORMATION
*****
IMPLICIT REAL*8 (A-H,O-Z)
COMMON/ IPARA/NUMNP,NUMEL,NGP,NCUR
DIMENSION XPT(1),YPT(1),ZPT(1),NUMPT(1),NREL(1),NCGT(20,1)
*** FOR OUTPUT OF GEOMETRY INFORMATION
WRITE(6,16)
16 FORMAT(//,5X,'GRID PCINT INFORMATION',//)

```

CEN04260
CEN04270
CEN04280
CEN04290
CEN04300
CEN04310
CEN04320
CEN04330
CEN04340
CEN04350
CEN04360
CEN04370
CEN04380
CEN04390
CEN04400
CEN04410
CEN04420
CEN04430
CEN04440
CEN04450
CEN04460
CEN04470
CEN04480
CEN04490
CEN04500
CEN04510
CEN04520
CEN04530
CEN04540
CEN04550
CEN04560
CEN04570
CEN04580
CEN04590
CEN04600
CEN04610
CEN04620
CEN04630
CEN04640
CEN04650
CEN04660
CEN04670
CEN04680
CEN04690
CEN04700
CEN04710
CEN04720
CEN04730

```

CEN04740
CEN04750
CEN04760
CEN04770
CEN04780
CEN04790
CEN04800
CEN04810
CEN04820
CEN04830
CEN04840
CEN04850
CEN04860
CEN04870
CEN04880
CEN04890
CEN04900
CEN04910
CEN04920
CEN04930
CEN04940
CEN04950
CEN04960
CEN04970
CEN04980
CEN04990
CEN05000
CEN05010
CEN05020
CEN05030
CEN05040
CEN05050
CEN05060
CEN05070
CEN05080
CEN05090
CEN05100
CEN05110
CEN05120
CEN05130
CEN05140
CEN05150
CEN05160
CEN05170
CEN05180
CEN05190
CEN05200
CEN05210

WRITE(6,17)
17 FORMAT(5X,'RESEQUENCED',4X,'USER INPUT'//
15X,'GRID POINT',5X,'GRID POINT'//
25X,'NUMBER',9X,'NUMBER',13X,'X',14X,'Y',14X,'Z'//)
DO 30 I=1,NUMNP
18 WRITE(6,18) I,NUMPT(I),XPT(I),YPT(I),ZPT(I)
20 FCORMAT(2X,I10,5X,I10,3X,3E15.4)
19 FCFORMAT(//,5X,'ELEMENT INFORMATION - WITH RESEQUENCED GRID PCINTS
1.//)
WRITE(6,9008)
9008 FCFORMAT(1X,'RESEQUENCED',4X,'USER INPUT',25X,'GRID PCINTS'//
11X,'ELEMENT',8X,'ELEMENT'//
21X,'NUMBER',9X,'NUMBER',7X,'1 2 3 4 5 6 7
3 8 9 10 11 12 13 14 15 16 17 18 19 20'//)
DO 40 I=1,NUMEL
9010 WRITE(6,9010)I,NREL(I),(NCONT(J,I),J=1,20)
40 FCFORMAT(1X,I4,11X,I4,9X,20I5)
CCNTINUE
959 RETURN
END
SUBROUTINE READIN(XPT,YPT,ZPT,NCCNT,NREL,NUMPT)
*****
SUBROUTINE TO READ ADINA DECK.
*****
IMPLICIT REAL*8 (A-H,O-Z)
REAL*4 TITLE(20)
COMMON/ IPARA/ NUMNP, NUMEL, NGP, NCUR
COMMON/ LOADS/ NLOAD, NLCUR, NPTM, IDGRAV
DIMENSION XPT(1), YPT(1), ZPT(1), NUMPT(1), NREL(1), NCONT(20,1)
1 CIMENTSION IDOF(6), ID(6), IDOLD(6), NODE(20), NFAR(20)
NP(20), INF(20)
DATA CTEST/,X
NCARD=0
READ(5,9000)(TITLE(I),I=1,20)
9011 WRITE(6,9011)(TITLE(I),I=1,20)
WFORMAT(//,5X,20A4,//)
READ MASTER CONTRCL CARDS
NUMNP = TOTAL NUMBER OF NODE POINTS
NREL = TOTAL NUMBER OF ELEMENT GROUPS
9011 ****
C ****
C ****
9001 NRELTY=NEGL+NEGL

```



```

K=K+KNOLC
XPT(K)=XFT(KK)+DX
IF(CT.NE.CTEST) GO TO 26
ROLD=ROLD+DR
DUMOLD=DUMOLD+DT
YPT(K)=ROLD*DCOS(DUMOLD)
ZPT(K)=ROLD*DSIN(DUMOLD)
GO TO 28
CONTINUE
YPT(K)=YFT(KK)+DY
ZPT(K)=ZPT(KK)+DZ
CONTINUE
NUMPT(K)=K
CONTINUE
NCLD=N
KNOLD=KN
DUMOLD=DUM
TC CGUNT DOFS TO DETERMINE NUMBER CF IC CARDS
DC 55 I=1,6
IF(IDOF(I).EQ.C.AND.ID(I).EQ.0) NEQ=NEQ+1
IDOLD(I)=ID(I)
CONTINUE
IF(N.NE.NUMPT) GO TO 10
READ LOAD CCONTROL CARDS
FCR MAT(415)
DC 80 I=1,IMASSN
IF(IMASSN.EQ.0) GO TO 81
READ(5,9C00) DUMMY
CONTINUE
CCONTINUE
IF(IDAMPN.EQ.0) GO TO 91
DC 90 I=1,ICAMPN
READ(5,9C00) DUMMY
CONTINUE
CONTINUE
READ IN INITIAL CONDITIONS
READ(5,9002) ICON
IF(ICON.EQ.0) GO TO 100
CARDNR=NEQ/6.0
NCARD=IDINT(CARDNR)
TEST=CARDNR-NCARD
IF(TEST.GT.C.1) NCARD=NCARD+1
DC 95 I=1,NCARD
READ(5,9C00) DUMMY
CONTINUE
95 IF(IMASSN.EQ.0) GO TO 100
DC 96 I=1,NCARD

```

CEN05700
CEN05710
CEN05720
CEN05730
CEN05740
CEN05750
CEN05760
CEN05770
CEN05780
CEN05790
CEN05800
CEN05810
CEN05820
CEN05830
CEN05840
CEN05850
CEN05860
CEN05870
CEN05880
CEN05890
CEN05900
CEN05910
CEN05920
CEN05930
CEN05940
CEN05950
CEN05960
CEN05970
CEN05980
CEN05990
CEN06000
CEN06010
CEN06020
CEN06030
CEN06040
CEN06050
CEN06060
CEN06070
CEN06080
CEN06090
CEN06100
CEN06110
CEN06120
CEN06130
CEN06140
CEN06150
CEN06160
CEN06170

CEN06660
CEN06670
CEN06680
CEN06690
CEN06700
CEN06710
CEN06720
CEN06730
CEN06740
CEN06750
CEN06760
CEN06770
CEN06780
CEN06790
CEN06800
CEN06810
CEN06820
CEN06830
CEN06840
CEN06850
CEN06860
CEN06870
CEN06880
CEN06890
CEN06900
CEN06910
CEN06920
CEN06930
CEN06940
CEN06950
CEN06960
CEN06970
CEN06980
CEN06990
CEN07000
CEN07010

```

6C
61      CONTINUE
      CC CONTINUE
      IF(NPAR(14).EQ.0) NPAR(14)=1
      NEL=NPAR(14)-1
130    READ(5,5002) INEL,IINC
9002    FCRMAT(15,30X,I5)
      IF(IINC.EQ.C) IINC=1
      READ(5,9004) (INP(I),I=1,8)
9004    READ(5,9004) (INP(I),I=9,N20)
14C    FCRMAT(12,15)
      NEL=NEL+1
      NREL(NEL)=NEL
      ML=INEL-NEL
      IF(ML) 150,155,160
150    WRITE(6,800C)NEL
800C    FCRMAT(//5X,'WARNING - ERROR IN ELEMENT ',I5//)
C *** NO GENERATION OF NCDE POINTS REQUIRED
155    CC 156 I=1,N20
      NP(I)=INP(I)
      NCONT(I,NEL)=NP(I)
156    CONTINUE
      CC TO 162
C *** GENERATION CF NODE PCINTS REQUIRED
160    DC 161 I=1,N20
      IF(NP(I).EQ.0) GO TO 161
      NP(I)=NP(I)+KN
      NCONT(I,NEL)=NP(I)
      CONTINUE
161    CC CONTINUE
162    NUMEL=NUMEL+1
      IF(NEL.EQ.NPAR(2)) RETURN
      IF(NEL.LT.INEL) GO TO 140
      KN=IINC
      GO TO 130
900    CONTINUE
      END

```

APPENDIX D

PROGRAM KCONT LISTING

```

*****
PROGRAM KCONT
THIS PROGRAM READS AN 8-20 NODE ADINA INPUT DECK AND
DETERMINES THE UNIDENTIFIED NCCE LOCATIONS TO YIELD
THE COORDINATES AND CONNECTIVITY FOR A 27 NCCE BRICK
MESH. THE OUTPUT IS PRINTED ON THE LINE PRINTER
AND WRITTEN ON USER DEFINED FILES 38 AND 59.
FILES:
FT58FC01-COORDINATES OF ALL NODES WRITTEN IN
SEQUENCE AS FOLLOWS: NCCE NUMBER,
X-COORDINATE, Y-COORDINATE, Z-COORDINATE.
FT59FC01-CONNECTIVITY ARRAY DIMENSIONED 27 BY
NUMEL. STORED IN SEQUENCE BY ROWS.
INPUT DATA REQUIREMENTS:
CARD 1
VARIABLE COLUMN REMARKS
NUMNP 1-10 NUMBER OF NODES IN INPUT
MESH.
NUMEL 11-20 NUMBER OF ELEMENTS IN INPUT
MESH
PLACE HERE THE ADINA INPUT DECK FROM THE TITLE CARD
TO THE LAST CONNECTIVITY CARD INCLUSIVE.
WRITTEN BY: L.R. EASTERLING NPS, MONTEREY CA., FEB 1978
*****
COMMON A(30000)
DATA A/30000*0/
COMMON/IPARA/NUMNP,NUMEL
READ(5,2000)NUMNP,NUMEL
FORMAT(2110)
MTOT=30000
N1=1
2000
*****
EAS00010
EAS00020
EAS00030
EAS00040
EAS00050
EAS00060
EAS00070
EAS00080
EAS00090
EAS00100
EAS00110
EAS00120
EAS00130
EAS00140
EAS00150
EAS00160
EAS00170
EAS00180
EAS00190
EAS00200
EAS00210
EAS00220
EAS00230
EAS00240
EAS00250
EAS00260
EAS00270
EAS00280
EAS00290
EAS00300
EAS00310
EAS00320
EAS00330
EAS00340
EAS00350
EAS00360
EAS00370
EAS00380
EAS00390
EAS00400
EAS00410

```



```

NN2=NUMNP
CC 30 I=1, NLMEL
NN2=NN2+1
DC 40 J=1, 2C
NCCN(J)=NCONT(J,I)
K=NCON(J)
CCD(J,1)=0.000
CCD(J,2)=0.000
CCD(J,3)=0.000
IF(K.EQ.0) GC TO 40
CCD(J,1)=XPT(K)
CCD(J,2)=YPT(K)
CCD(J,3)=ZPT(K)
CCNTINUE
40 CALL ADCRD(R,S,T,COD,NCON,I,XX,YY,ZZ)
XFT(NN2)=XX
YPT(NN2)=YY
ZPT(NN2)=ZZ
3C KCCNT(21,I)=NN2
DC 50 I=1, NLMEL
CC 50 J=1, 6
NFACE(J,I)=C.000
DC 50 K=1, 4
L=IFACE(K,J)
50 NFACE(J,I)=NFACE(J,I)+KCONT(L,I)
DC 3000 I=1, NLMEL
DC 3000 J=1, 12
I1=ILINE(1,J)
I2=ILINE(2,J)
3000 NLINE(J,I)=KCONT(I1,I)+KCONT(I2,I)
DC 70 I=1, NLMEL
DC 70 J=1, 15
K=NORD(J)
IF(KCONT(K,I).NE.0) GO TO 70
NN2=NN2+1
R=CNAT(1,J)
S=CNAT(2,J)
T=CNAT(3,J)
DC 80 M=1, 2C
CCC(M,1)=0.000
CCC(M,2)=0.000
CCD(M,3)=0.000
NCCN(M)=NCONT(M,I)
IF(N.EQ.0) GC TO 80
CCD(M,1)=XPT(N)
CCD(M,2)=YPT(N)
CCD(M,3)=ZPT(N)

```

```

EAS00910
EAS00920
EAS00930
EAS00940
EAS00950
EAS00960
EAS00970
EAS00980
EAS00990
EAS01000
EAS01010
EAS01020
EAS01030
EAS01040
EAS01050
EAS01060
EAS01070
EAS01080
EAS01090
EAS01100
EAS01110
EAS01120
EAS01130
EAS01140
EAS01150
EAS01160
EAS01170
EAS01180
EAS01190
EAS01200
EAS01210
EAS01220
EAS01230
EAS01240
EAS01250
EAS01260
EAS01270
EAS01280
EAS01290
EAS01300
EAS01310
EAS01320
EAS01330
EAS01340
EAS01350
EAS01360
EAS01370

```

AD-A056 310

NAVAL POSTGRADUATE SCHOOL MONTEREY CALIF
STRESS ANALYSIS OF CERAMIC TURBINE BLADES BY FINITE ELEMENT MET--ETC(U)
MAR 78 L R EASTERLING
NPS69-78-009

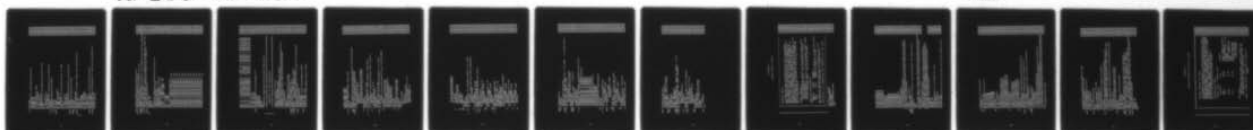
F/G 21/5

UNCLASSIFIED

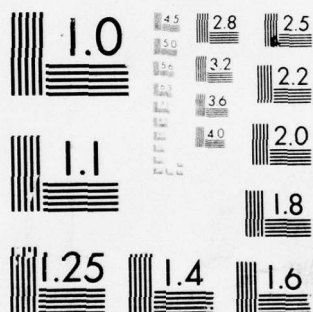
NL

2 OF 2

AD
A066310



END
DATE
FILMED
8-78
DDC



```

8C  CCNTINUE
   CALL ADCRD(R,S,T,COD,NCON,I,XX,YY,ZZ)
   XPT(NN2)=XX
   YPT(NN2)=YY
   ZPT(NN2)=ZZ
   IF(K.LE.20)GO TO 5000
   DC 90 I=1,NUMEL
   DC 90 J=1,6
   KK=NORD(JJ+13)
   IF(NFACE(JJ,II).NE.NFACE(J-13,I))GG TO 90
   KTR=0
   DC 111 L=1,4
   LL=IFACE(L,J-13)
   DC 111 MM=1,8
   IF(KCONT(MM,II).EQ.KCCNT(LL,I))KTR=KTR+1
   CCNTINUE
111  IF(KTR.EQ.4)KCONT(KK,II)=NN2
   CCNTINUE
   GC TO 70
5000  CCNTINUE
      II=1,NUMEL
      DC 4000 J5=1,12
      DC 4000 J=1,12
      KK=NORD(J5)
      IF(NLINE(J5,II).NE.NLINE(J,I))GC 7C 4000
      KTR=0
      DC 4001 L=1,2
      LL=ILINE(L,J)
      DC 4001 MM=1,8
      IF(KCONT(MM,II).EQ.KCCNT(LL,I))KTR=KTR+1
      CCNTINUE
4001  IF(KTR.EQ.2)KCONT(KK,II)=NN2
      CCNTINUE
4000  CCNTINUE
      WRITE(6,1003)NN2
1003  FCFORMAT(/5X,17,' DISTINCT POINTS ARE IDENTIFIED'//)
      C
      C
      C
      REWIND 58
      REWIND 59
      WRITE(58)NN2
      WRITE(6,1006)
      DC 100 I=1,NUMEL
      WRITE(6,1001)I
      DC 100 J=1,27
      K=KCONT(J,I)
      WRITE(6,1002)J,K,XPT(K),YPT(K),ZPT(K)
100  WRITE(6,1004)
1004  FCFORMAT(/5X,'NODE COORDINATES BY NCDE NR',//5X,'NODE',5X,
      1CCCOORDINATES',//)
      DC 666 I=1,NN2

```

```

666 WRITE(6,1005)I,XPT(I),YPT(I),ZPT(I)
C 666 WRITE(58)I,XPT(I),YPT(I),ZPT(I)
C 666 WRITE(59)((KCONT(I,J),J=1,NUMEL),I=1,27)
1005 FCRMAT(IX,IS,3F16.5)
1000 FCRMAT(//5X,NODE CCORDINATES PLUS CENTROIC AND MID-FAC COORDINATES BY ELEMENT,////)
1001 FCRMAT(5X,AR,8X,X-COORD,8X,Y-COORD,8X,Z-COORD,8X,COORD NR,
1002 FCRMAT(5X,2I10,3F15.5)
C
C
END
SLBROUTINE ADCRD(R,S,T,COD,NCON,IEL,XX,YY,ZZ)
IMPLICIT REAL*8(A-T,O-Z)
DIMENSION EMI(20)
DIMENSION COD(20,3),PROD1(3)
DIMENSION NCON(20)
GF(BT) = 0.5D0*(1.0D0 + BT)
GM(BT) = 0.5D0*(1.0D0 - BT)
GZ(BT) = 1.0D0 - BT*BT
ZRO = 0.0D0
ONE = 1.0D0
TWO = 2.0D0
EMI( 9) = GZ(R)*GP(S)*GP(T)
IF(NCON( 9).EQ.0) EMI( 9) = ZRO
EMI(10) = GM(R)*GZ(S)*GP(T)
IF(NCON(10).EQ.0) EMI(10) = ZRO
EMI(11) = GZ(R)*GM(S)*GP(T)
IF(NCON(11).EQ.0) EMI(11) = ZRO
EMI(12) = GP(R)*GZ(S)*GP(T)
IF(NCON(12).EQ.0) EMI(12) = ZRO
EMI(13) = GZ(R)*GP(S)*GM(T)
IF(NCON(13).EQ.0) EMI(13) = ZRO
EMI(14) = GM(R)*GZ(S)*GM(T)
IF(NCON(14).EQ.0) EMI(14) = ZRO
EMI(15) = GZ(R)*GM(S)*GM(T)
IF(NCON(15).EQ.0) EMI(15) = ZRO
EMI(16) = GP(R)*GZ(S)*GM(T)
IF(NCON(16).EQ.0) EMI(16) = ZRO
EMI(17) = GP(R)*GP(S)*GZ(T)
IF(NCON(17).EQ.0) EMI(17) = ZRO
EMI(18) = GM(R)*GP(S)*GZ(T)
IF(NCON(18).EQ.0) EMI(18) = ZRO
EMI(19) = GM(R)*GM(S)*GZ(T)
IF(NCON(19).EQ.0) EMI(19) = ZRO
EMI(20) = GP(R)*GM(S)*GZ(T)
IF(NCON(20).EQ.0) EMI(20) = ZRO

```


EA S02820
EA S02830
EA S02840
EA S02850
EA S02860
EA S02870
EA S02880
EA S02890
EA S02900
EA S02910
EA S02920
EA S02930
EA S02940
EA S02950
EA S02960
EA S02970
EA S02980
EA S02990
EA S03000
EA S03010
EA S03020
EA S03030
EA S03040
EA S03050
EA S03060
EA S03070
EA S03080
EA S03090
EA S03100
EA S03110
EA S03120
EA S03130
EA S03140
EA S03150
EA S03160
EA S03170
EA S03180
EA S03190
EA S03200
EA S03210
EA S03220
EA S03230
EA S03240
EA S03250
EA S03260
EA S03270
EA S03280
EA S03290

```

C ***
      READ(5,9000) DUMMY
      READ(5,9000) DUMMY
      READ(5,9000) DUMMY
      NCLD=0
      NEQ=0
      10 READ(5,9006) CT,N, (ID(I),I=1,6),XPT(N),YPT(N),ZPT(N),KN
      9006 FORMAT(1,14,1X,14,5I5,3F10.0,15)
      C ***
      CHECK FOR CYLINDRICAL COORDINATES
      IF(CT.NE.CTEST) GC TO 12
      DUM=ZPT(N)/57.2958
      R=YPT(N)
      YPT(N)=R*DCOS(ZPT(N)/57.2958D0)
      ZPT(N)=R*DSIN(ZPT(N)/57.2958D0)
      12 CONTINUE
      NLMP(T(N)=N
      IF(NOLD.EQ.0) GO TC 50
      C ***
      FOR GENERATION OF FIXED BOUNDARY CONDITIONS
      15 I=1,6
      IF(IDOLD(I).EQ.-1.AND.ID(I).EQ.0) ID(I)=ICOLD(I)
      CONTINUE
      IF(KNOLD.EQ.0) GO TO 50
      NLN=(N-NOLD)/KNOLD
      NLN=NLN-1
      IF(NLNM.LT.1) GO TC 50
      C ***
      TC COUNT DOFS TO DETERMINE NUMBER CF IC CARCS
      20 I=1,6
      IF(IDDF(I).EQ.0.AND.IDOLD(I).EQ.0) NEQ=NEQ+NLNM
      CONTINUE
      CX=(XPT(N)-XPT(NOLD))/NUM
      IF(CT.NE.CTEST) GO TO 21
      RCLD=YPT(NOLD)/DCOS(DUMOLD)
      RNEW=YPT(N)/DCOS(CUM)
      CR=(RNEW-ROLD)/NUM
      CT=(CUM-DUMOLD)/NLN
      GC TO 22
      21 CONTINUE
      CY=(YPT(N)-YPT(NOLD))/NUM
      DZ=(ZPT(N)-ZPT(NOLD))/NUM
      22 CCNTINUE
      K=NCLD
      DC 30 J=1,NLMN
      KK=K
      K=K+KNOLD
      XPT(K)=XPT(KK)+DX
      IF(CT.NE.CTEST) GO TO 26
      ROLD=ROLD+DR
      DUMOLD=DUMOLD+DT

```



```

EAS033320
EAS033330
EAS033340
EAS033350
EAS033360
EAS033370
EAS033380
EAS033390
EAS033400
EAS033410
EAS033420
EAS033430
EAS033440
EAS033450
EAS033460
EAS033470
EAS033480
EAS033490
EAS033500
EAS033510
EAS033520
EAS033530
EAS033540
EAS033550
EAS033560
EAS033570
EAS033580
EAS033590
EAS033600
EAS033610
EAS033620
EAS033630
EAS033640
EAS033650
EAS033660
EAS033670
EAS033680
EAS033690
EAS033700
EAS033710
EAS033720
EAS033730
EAS033740
EAS033750
EAS033760
EAS033770

```

```

26 YPT(K)=ROLD*DCCS(DUMOLD)
    ZPT(K)=ROLD*DSIN(DUMOLD)
    GO TO 28
    CONTINUE
28 YPT(K)=YPT(KK)+DY
    ZPT(K)=ZPT(KK)+DZ
    CONTINUE
30 NUMPT(K)=K
    CONTINUE
5C NCILD=N
    KNCLD=KN
    DUMOLD=DUM
    TC COUNT DOFS TO DETERMINE NUMBER CF IC CARCS
    DC 55 I=1,6
    IF(IDOF(I).EQ.0.AND.ID(I).EQ.C) NEQ=NEQ+1
    IF(IDOF(I)=ID(I))
    CONTINUE
55 IF(N.NE.NUMAP) GO TO 10
    READ LOAD CCNTROL CARCS
    FCFORMAT(415)
    DC 80 I=1,IMASSN
    IF(IMASSN.EQ.C) GO TO 81
    IF(READ(5,9000) DUMMY
    CONTINUE
8C CONTINUE
81 IF(IDAMPN-EC.C) GC TO 91
    DC 90 I=1,ICAMPN
    READ(5,9000) DUMMY
    CONTINUE
90 CONTINUE
51 READ INITIAL CONDITIONS
    READ(5,9002) ICON
    IF(ICON.EQ.C) GO TC 100
    CARONR=NEQ/6.C
    NCARD=IDINT(CARDNR)
    IF(TEST.GT.C.1) NCARD=NCARD+1
    DC 95 I=1,NCARD
    READ(5,9000) DUMMY
    CONTINUE
55 IF(IMASS.EQ.C) GO TO 103
    DC 96 I=1,NCARD
    READ(5,9000) DUMMY
    CONTINUE
56 CC 98 I=1,NCARD
    READ(5,9000) DUMMY
    CONTINUE
58

```

EAS03780
 EAS03790
 EAS03800
 EAS03810
 EAS03820
 EAS03830
 EAS03840
 EAS03850
 EAS03860
 EAS03870
 EAS03880
 EAS03890
 EAS03900
 EAS03910
 EAS03920
 EAS03930
 EAS03940
 EAS03950
 EAS03960
 EAS03970
 EAS03980
 EAS03990
 EAS04000
 EAS04010
 EAS04020
 EAS04030
 EAS04040
 EAS04050
 EAS04060
 EAS04070
 EAS04080
 EAS04090
 EAS04100
 EAS04110
 EAS04120
 EAS04130
 EAS04140
 EAS04150
 EAS04160
 EAS04170
 EAS04180
 EAS04190
 EAS04200
 EAS04210
 EAS04220
 EAS04230
 EAS04240
 EAS04250

```

9007 FCRMAT(6E12.6)
100 CCNTINUE
    NMEL=0
    WRITE(6,9005) NEQ,NCARD
9005 FCRMAT(///,NEQ AND NCARD FOR IC IN GEOM1 = ',15,10X,15///)
C *** READ ELEMENT CONTRL CARDS
    DO 900 M=1,NELTYP
      READ(5,9008)(NPAR(I),I=1,20)
9008 FCRMAT(2014)
9010 FCRMAT(///,NPAR = ',2015///)
      MTYPE=NPAR(1)
      NUMMAT=NPAR(16)
      NSTRES=NPAR(13)
C *** CALCULATE THE NUMBER OF MATERIAL CASE CARDS
      IF(NPAR(15).EQ.1) NCARD=1
      IF(NPAR(15).EQ.2) NCARD=2+NPAR(18)
      IF(NPAR(15).EQ.3) NCARD=4
      IF(NPAR(15).EQ.4) NCARD=2
      IF(NPAR(15).EQ.5) NCARD=1
      IF(NPAR(15).EQ.8) NCARD=1
      IF(NPAR(15).EQ.9) NCARD=1
      IF(NPAR(15).EQ.10) NCARD=6
      IF(NPAR(15).EQ.11) NCARD=6
      IF(NPAR(15).NE.12) GC TO 111
      CARDNR=NPAR(17)/8.0
      NCARD=ICINT(CARDNR)
      TEST=CARDNR-NCARD
      IF(TEST.GT.C.1) NCARD=NCARD+1
111 CCNTINUE
    N20=20
C *** READ MATERIAL PROPERTIES
    DO 222 J=1,NUMMAT
      READ(5,9000) DUMMY
9000 FCRMAT(2044)
      DO 45 I=1,NCARD
        READ(5,9000) DUMMY
        CCNTINUE
45 CCNTINUE
C *** READ STRESS OUTPUT TABLE CARDS
    IF(NPAR(13).EQ.0) GO TO 61
    DO 60 I=1,NSTRES
      READ(5,9000) DUMMY
      CCNTINUE
60 CCNTINUE
61 CONTINUE
    IF(NPAR(14).EQ.0) NPAR(14)=1
    NEL=NPAR(14)-1
120 READ(5,9002) INEL,IINC
  
```

EAS04260
 EAS04270
 EAS04280
 EAS04290
 EAS04300
 EAS04310
 EAS04320
 EAS04330
 EAS04340
 EAS04350
 EAS04360
 EAS04370
 EAS04380
 EAS04390
 EAS04400
 EAS04410
 EAS04420
 EAS04430
 EAS04440
 EAS04450
 EAS04460
 EAS04470
 EAS04480
 EAS04490
 EAS04500
 EAS04510
 EAS04520
 EAS04530
 EAS04540
 EAS04550
 EAS04560

```

9002 FFORMAT(15,3CX,15)
    IF(I,INC,EQ,C) IINC=1
    READ(5,5004) (INP(I),I=1,8)
    READ(5,9004) (INP(I),I=9,N20)
9004 FFORMAT(12I5)
140  NEL=NEL+1
    NREL(NEL)=NEL
    ML=INL-NEL
    IF(ML) 150,155,160
150  WRITE(6,8000)NEL
8000 FFORMAT(//5X,'WARNING - ERROR IN ELEMENT ',I5//)
C *** NC GENERATION OF NCDE POINTS REQUIRED
155  DC 156 I=1,N20
    NP(I)=INP(I)
    NCUNT(I,NEL)=NP(I)
    CONTINUE
156  GC TO 162
C *** GENERATION CF NODE PCINTS REQUIRED
160  DC 161 I=1,N20
    IF(NP(I).EQ.0) GO TO 161
    NP(I)=NP(I)+KA
    NCUNT(I,NEL)=NP(I)
    CONTINUE
161  CCNTINUE
162  NCMEL=NCMEL+1
    IF(NEL.EQ.NFAR(2)) RETURN
    IF(NEL.LT.INEL) GO TO 140
    KN=IINC
    GC TO 130
900  CONTINUE
    END
  
```

APPENDIX E

PROGRAM STRESS LISTING

```

** ** ** ** ** ** ** ** ** ** ** ** ** ** ** ** ** ** ** ** ** ** ** ** ** ** ** ** ** ** ** ** ** ** ** ** ** **  PROGRAM STRESS
** ** ** **  THIS PROGRAM TAKES THE CONNECTIVITY DATA FROM PROGRAM
** ** ** **  KCONT AND THE STRESS RESULTS FROM AN ACINA ANALYSIS WITH
** ** ** **  THE 27 NODE BRICK CUTOPT OPTION USED AND AVERAGES THE
** ** ** **  CONTRIBUTIONS TO EACH NODE BY THE VARIOUS ELEMENTS TO
** ** ** **  WHICH IT IS A MEMBER. THESE VALUES ARE THEN OPERATED ON
** ** ** **  TO YIELD THE THREE PRINCIPAL STRESSES AND AN ARRAY
** ** ** **  CONTAINING THE MAXIMUM PRINCIPAL STRESS FOR EACH NODE. THE
** ** ** **  OUTPUT CONSISTS OF A LINE PRINTER LISTING OF AVERAGE AND
** ** ** **  PRINCIPAL STRESSES AND STORAGE CN USER DEFINED FILES 60
** ** ** **  AND 61 RESPECTIVELY.
** ** ** **  OUTPUT STORAGE:
** ** ** **  FT60FCI-SEQUENTIAL LISTING OF THE AVERAGE STRESS ARRAYS
** ** ** **  IN THE FOLLOWING ORDER: ASIGX,ASIGY,ASIGZ,ATALXY,
** ** ** **  ATALYZ,ATAUZY.
** ** ** **  FT61FCI-SEQUENTIAL LISTING OF THE PRINCIPAL STRESS ARRAY
** ** ** **  IN THE FOLLOWING ORDER: PSIG1,PSIG2,PSIG3,PMAX.
** ** ** **  INPUT DATA REQUIREMENTS:
** ** ** **  CARD 1      C COLUMN      REMARKS
** ** ** **  VARIABLE   1-5          NUMBER OF NODES IN 27 NODE BRICK MESH
** ** ** **  NN2        6-10        NUMBER OF ELEMENTS IN MESH
** ** ** **  NUMEL                  NUMBER OF ELEMENTS IN MESH
** ** ** **  CD CARDS ARE REQUIRED FOR FILE 57 ESTABLISHED BY ACINA
** ** ** **  AND FILES 58 AND 59 ESTABLISHED BY PROGRAM KCONT.
** ** ** **  WRITTEN BY: L.R. EASTERLING NPS, MONTEREY CA., FEB 1978
** ** ** **  DIMENSION A(68000)
** ** ** **  DATA A/68000*0./
** ** ** **  MIGT=68000
** ** ** **  READ(5,1000)NN2,NUMEL
** ** ** **  N1=1

```

STR00010
STR00020
STR00030
STR00040
STR00050
STR00060
STR00070
STR00080
STR00090
STR00100
STR00110
STR00120
STR00130
STR00140
STR00150
STR00160
STR00170
STR00180
STR00190
STR00200
STR00210
STR00220
STR00230
STR00240
STR00250
STR00260
STR00270
STR00280
STR00290
STR00300
STR00310
STR00320
STR00330
STR00340
STR00350
STR00360
STR00370
STR00380
STR00390
STR00400

CC


```

1  TAUXZ(J,IEL),TAUYZ(J,IEL)
10  CONTINUE
20  READ(58)J,(CCD(K,J),K=1,3)
30  DC 30 I=1,NN2
    ASIGX(I)=0.0D0
    ASIGY(I)=0.0D0
    ASIGZ(I)=0.0D0
    ATAUXY(I)=0.0D0
    ATAUZ(I)=0.0D0
    ATAUZ(I)=0.0D0
    KTR(I)=0
40  CC 40 I=1,NLMEL
    CC 40 J=1,27
    K=KCONT(J,I)
    ASIGX(K)=ASIGX(I)+SIGX(J,I)
    ASIGY(K)=ASIGY(I)+SIGY(J,I)
    ASIGZ(K)=ASIGZ(I)+SIGZ(J,I)
    ATAUXY(K)=ATAUXY(I)+TAUXY(J,I)
    ATAUZ(K)=ATAUZX(K)+TAUZX(J,I)
    ATAUZ(K)=KTR(K)+1
50  CC 50 I=1,NN2
    ASIGX(I)=ASIGX(I)/KTR(I)
    ASIGY(I)=ASIGY(I)/KTR(I)
    ASIGZ(I)=ASIGZ(I)/KTR(I)
    ATAUXY(I)=ATAUXY(I)/KTR(I)
    ATAUZ(I)=ATAUZX(I)/KTR(I)
60  REWIND 60
1001 WRITE(60)ASIGX,ASIGY,ASIGZ,ATAUXY,ATAUXZ,ATAUYZ
    WRITE(6,1001)
    FCFORMAT(//)5X,'AVERAGED NODAL STRESSES'////)
    CC 60 I=1,NN2
    WRITE(6,1000)I,ASIGX(I),ASIGY(I),ASIGZ(I),ATAUXY(I),
1  ATAUZ(I),ATAUYZ(I)
60  CONTINUE
1000 FCFORMAT(1X,I6,F16.5)
    CTHRD=1.0D0/3.0D0
    PI=.141592654
    DC 100 I=1,NN2
    P=-(ASIGX(I)+ASIGY(I)+ASIGZ(I))
    Q=ASIGX(I)*ASIGY(I)+ASIGY(I)*ASIGZ(I)+ASIGX(I)*ASIGZ(I)
1  R=-(ATAUXY(I)+ATAUZX(I)+ATAUYZ(I))*2-ATAUXZ(I)*ATAUYZ(I)
1  R=-(ASIGX(I)+ASIGY(I)+ASIGZ(I))*2-ATAUXZ(I)*ATAUYZ(I)
22) A=(3.0D0*(-P**2)/3.0D0

```

```

STR0C890
STR0C900
STR0C910
STR00920
STR00930
STR00940
STR00950
STR00960
STR00970
STR00980
STR00990
STR01000
STR01010
STR01020
STR01030
STR01040
STR01050
STR01060
STR01070
STR01080
STR01090
STR01100
STR01110
STR01120
STR01130
STR01140
STR01150
STR01160
STR01170
STR01180
STR01190
STR01200
STR01210
STR01220
STR01230
STR01240
STR01250
STR01260
STR01270
STR01280
STR01290
STR01300
STR01310
STR01320
STR01330
STR01340
STR01350
STR01360

```

```

R=(2.000*P**3-9.000*P*Q+27.000*R)/27.000
AB=(B**2)/4.000+(A**3)/27.000
IF(AB)400,300,200
WRITE(6,2000)I,AB,A,B,P,Q,R
200 PSIG1(I)=1111111.
PSIG2(I)=PSIG1(I)
PSIG3(I)=PSIG1(I)
GC TO 100
300 AA=(-B/2.000)**0.5THRD
BE=AA
PSIG1(I)=AA*2.000-P/3.000
PMAX(I)=PSIG1(I)
PSIG2(I)=-AA-P/3.000
PSIG3(I)=PSIG2(I)
IF(PSIG2(I).GT.PSIG1(I))PMAX(I)=PSIG2(I)
GC TO 100
400 PHI=DARCCOS((-B/2.000)/DSQRT((-A**3)/27.000))
PSIG1(I)=2.000*DSQRT(-A/3.000)*DCCS(PHI/3.000)-P/3.000
PSIG2(I)=2.000*DSQRT(-A/3.000)*DCCS(PHI/3.000*PI/3.000)
1-PSIG3(I)=2.000*DSQRT(-A/3.000)*DCCS(PHI/3.000*PI/3.000)
1-PSIG3(I)=2.000*DSQRT(-A/3.000)*DCCS(PHI/3.000*PI/3.000)
1-PSIG3(I)=2.000*DSQRT(-A/3.000)*DCCS(PHI/3.000*PI/3.000)
PMAX(I)=PSIG1(I)
IF(PSIG2(I).GT.PMAX(I))PMAX(I)=PSIG2(I)
IF(PSIG3(I).GT.PMAX(I))PMAX(I)=PSIG3(I)
100 CONTINUE
REWINDD 61
WRITE(6,2001)
CC 600 I=1,AN2
600 WRITE(6,2002)I,PMAX(I),PSIG1(I),PSIG2(I),PSIG3(I)
2000 FCRMAT(//5X,SOLUTICA FCR NCDE,15,IS,IMAGINARY,//
1 10X,AB=,G25.16/10X,A=,G25.16/10X,B=,G25.16/
2 10X,P=,G25.16/10X,Q=,G25.16/10X,R=,G25.16/10X)
2001 FCRMAT(//20X,NODAL PRINCIPAL STRESS FOR FIRST STAGE ROTCR ELADE
1 //5X,NODE,5X,MAXIMUM,13X,NR 1,16X,NR 2,16X,NR 3,/)
2002 FCRMAT(1X,1E,5X,4G20.11)
ENDFILE 60
RETURN
END

```

STR01370
 STR01380
 STR01390
 STR01400
 STR01410
 STR01420
 STR01430
 STR01440
 STR01450
 STR01460
 STR01470
 STR01480
 STR01490
 STR01500
 STR01510
 STR01520
 STR01530
 STR01540
 STR01550
 STR01560
 STR01570
 STR01580
 STR01590
 STR01600
 STR01610
 STR01620
 STR01630
 STR01640
 STR01650
 STR01660
 STR01670
 STR01680
 STR01690
 STR01700
 STR01710
 STR01720
 STR01730
 STR01740
 STR01750
 STR01760
 STR01770

APPENDIX F

PROGRAM CONTOUR PLOT DATA LISTING

```

*****
PROGRAM CCNTCUR PLGT DATA
THIS PROGRAM IS DESIGNED TO TAKE NCCLAL PCINT DATA FROM
AN ADINA 3-D MESH FROM FILE 58 OF PROGRAM KCCNT AND PLOT
NODE LOCATION MARKS AND NODE NUMBERS FOR VARIOUS DESIRED
2-DIMENSIONAL PLANES. PLANES MAY BE DEFINED BY SPECIFIC
COORDINATE VALUE, LIMITING COORDINATE VALUES, OR INPUT
OF DESIRED NODE NUMBERS TO BE PLOTTED.
DATA FOR CONTOUR PLOTTING CAN ALSO BE OUTPUT
ON THE LINE PRINTER AND/OR PUNCHED CARDS.

REQUIRED DATA DECK:
CONTROL CARD 1 (FORMAT 4110)

VARIABLE      COL
NN2            1-10
NPIC           11-20
NDMAX          21-30
VPCH           31-40

REMARKS
TOTAL NUMBER OF NCES
TOTAL NUMBER OF
DIFFERENT PLANES TO BE
PLOTTED
HIGHEST NUMBER OF
NCES EXPECTED PER
PLANE
FLAG FOR PUNCHING
CONTOUR PLOT DATA
0 FOR PLNCHING
1 FOR NO PUNCH

NODE CARDS
INPUT NPIC SETS OF CARDS. LEAVE COLUMNS FOR
TESTL, TESTH, ICRD BLANK IF NODES TO BE READ IN.
FOR EQUALITY TEST INPUT TESTL=TESTH.

CARD1 (FORMAT 20A4) TITLE CARD FOR ANALYSIS
PLANE.
*****
CTRP00010
CTRP00020
CTRP00030
CTRP00040
CTRP00050
CTRP00060
CTRP00070
CTRP00080
CTRP00090
CTRP00100
CTRP00110
CTRP00120
CTRP00130
CTRP00140
CTRP00150
CTRP00160
CTRP00170
CTRP00180
CTRP00190
CTRP00200
CTRP00210
CTRP00220
CTRP00230
CTRP00240
CTRP00250
CTRP00260
CTRP00270
CTRP00280
CTRP00290
CTRP00300
CTRP00310
CTRP00320
CTRP00330
CTRP00340
CTRP00350
CTRP00360
CTRP00370
CTRP00380
CTRP00390
CTRP00400

```

[illegible]


```

CCCCC
MAIN PROGRAM TO DETERMINE
DIMENSIONS AND CALL SUB-
ROUTINES
*****
CIMENSION A(26000)
COMMON/ IPARA/ NPCH
MTCT=26000
READ(5,1000) NN2, NPIC, NDMAX, NPCH
N1=1
N2=N1+NN2*2
N3=N2+NN2*2
N4=N3+NN2*2
N5=N4+NN2*2
N6=N5+NN2*2
N7=N6+NN2*2
N8=N7+NN2*2
N9=N8+NDMAX*NPIC
N10=N9+3*NN2
N11=N10+NPIC
N12=N11+3*NN2
N13=N12+NPIC*20
NLAST=N13+2*NPIC
IF(NLAST.GT.MTOT) GO TO 111
CALL DEFPLT (A(N1),A(N2),A(N3),A(N4),A(N5),A(N6),A(N7),
1A(N8),A(N9),A(N10),A(N11),A(N12),A(N13),NN2,NPIC,NDMAX)
STOP
111 WRITE(6,2000) NLAST
2000 FFORMAT(//1X,'NLA= ',110,'MTCT INSUFFICIENT'///)
1000 FFORMAT(4110)
STOP
END
*****
SUBROUTINE TO DEVELOP ANAL-
YSIS PLANES AND CALL PLOT
ROUTINE
*****
SUBROUTINE DEFPLT (XX,YY,ZZ,SIG1,SIG2,SIG3,SIGMX,LVL,COORD,KTR,
1PCOORD,TITLE,MC,NN2,NPIC,NDMAX)
REAL*8 XX(1),YY(1),ZZ(1),SIG1(1),SIG2(1),SIG3(1),SIGMX(1)
DIMENSION LVL(NPIC,1),COORD(NN2,1),FCCCRD(NN2,1)
DIMENSION TITLE(NPIC,1),MC(2,1)

```

```

CTRP0890
CTRP0900
CTRP0910
CTRP0920
CTRP0930
CTRP0940
CTRP0950
CTRP0960
CTRP0970
CTRP0980
CTRP0990
CTRP1000
CTRP1010
CTRP1020
CTRP1030
CTRP1040
CTRP1050
CTRP1060
CTRP1070
CTRP1080
CTRP1090
CTRP1100
CTRP1110
CTRP1120
CTRP1130
CTRP1140
CTRP1150
CTRP1160
CTRP1170
CTRP1180
CTRP1190
CTRP1200
CTRP1210
CTRP1220
CTRP1230
CTRP1240
CTRP1250
CTRP1260
CTRP1270
CTRP1280
CTRP1290
CTRP1300
CTRP1310
CTRP1320
CTRP1330
CTRP1340
CTRP1350
CTRP1360

```


CTRP1370
 CTRP1380
 CTRP1390
 CTRP1400
 CTRP1410
 CTRP1420
 CTRP1430
 CTRP1440
 CTRP1450
 CTRP1460
 CTRP1470
 CTRP1480
 CTRP1490
 CTRP1500
 CTRP1510
 CTRP1520
 CTRP1530
 CTRP1540
 CTRP1550
 CTRP1560
 CTRP1570
 CTRP1580
 CTRP1590
 CTRP1600
 CTRP1610
 CTRP1620
 CTRP1630
 CTRP1640
 CTRP1650
 CTRP1660
 CTRP1670
 CTRP1680
 CTRP1690
 CTRP1700
 CTRP1710
 CTRP1720
 CTRP1730
 CTRP1740
 CTRP1750
 CTRP1760
 CTRP1770
 CTRP1780
 CTRP1790
 CTRP1800
 CTRP1810
 CTRP1820
 CTRP1830
 CTRP1840

```

CCMMCN/IPARA/NPCH
DC 10 I=1,NPCT
KTR(I)=0
DC 10 J=1,NMAX
LVL(I,J)=0
10 READ(58)DUM
CC 20 I=1,NN2
20 READ(58)IDUM,XX(I),YY(I),ZZ(I)
DC 35 I=1,NN2
CCGRD(I,1)=XX(I)
CCORD(I,2)=YY(I)
CCCRD(I,3)=ZZ(I)
CCNTINUE
DC 30 I=1,NPCT
25 READ(5,1002)(TITLE(I,J),JJ=1,20)
1002 FCRMAT(20A4)
1000 READ(5,1000)TESTL,TESTH,ICRD,IRD,ICT,MC(1,I),MC(2,I)
1000 FCRMAT(2F10.0,5I5)
IF(IRD.EQ.1)GO TO 111
DC 40 J=1,NN2
IF(COORD(J,ICRD).GT.TESTL.AND.COORD(J,ICRD).LT.TESTH.OR.
1CCORD(J,ICRD).EQ.TESTL)GO TO 222
GC TO 40
222 KTR(I)=KTR(I)+1
K=KTR(I)
LVL(I,K)=J
40 CCNTINUE
GC TO 30
111 READ(5,1001)(LVL(I,L),L=1,ICT)
1001 FCRMAT(16I5)
KTR(I)=ICT
30 CCNTINUE
WRITE(6,200C)
DC 45 I=1,NPCT
K=KTR(I)
45 WRITE(6,2001)I,(LVL(I,J),J=1,K)
CALL MYPLOT(LVL,COORD,KTR,PCOORD,MC,NN2,NPCT,NMAX)
CALL PLTDT(SIG1,SIG2,SIG3,SIGMX,LVL,COORD,KTR,TITLE,MC,
1NN2,NPCT)
2000 FCRMAT(//5X,'NODES NUMBERS BY ANALYSIS PLANE'///)
2001 FCRMAT(//5X,'PLANE NR ',15//1X,4(1X,25I5//)
      RETURN
      END
  
```

CCC

```

C
C
C
SUBROUTINE TC PLCT ANALYSIS PLANES
*****
SUBROUTINE MYPLOT(LVL,COORD,KTR,PCCORD,MC,NN2,NP1CT,NDMAX)
DIMENSION LVL(NP1CT,1),KTR(1),PCCORD(NN2,1),PCCCRD(NN2,1)
DIMENSION TITLE1(20)
DIMENSION MC(2,1)
COMMON/ IPARA/NPCH
READ(5,1000)(TITLE1(I),I=1,20)
CC 10 I=1,NN2
CC 10 J=1,3
10 PCCORD(I,J)=COORD(I,J)*DMAGS
CALL PLOTS
CALL PLOT(-12.,3.,-3)
CALL PLOT(1.,0.,-3)
CALL SYMBOL(0.,0.,14,TITLE1,0.,8C)
CALL PLOT(4.25,5.25,-3)
CC 20 I=1,NP1CT
MX=MC(1,1)
MY=MC(2,1)
K=KTR(1)
CC 30 J=1,K
L=LVL(I,J)
X=PCOORD(L,MX)-.02
Y=PCOORD(L,MY)-.035
CALL SYMBOL(X,Y,.07,'X',0.,1)
X=X+.06
Y=Y-.035
F=FLOAT(L)
CALL NUMBER(X,Y,.14,F,0.,-1)
30 CCNTINUE
CALL PLCT(-4.25,5.,-3)
CALL SYMBOL(0.,0.,14,'LEVEL',0.,5)
F=FLOAT(I)
CALL NUMBER(1.,0.,0.,14,F,0.,-1)
CALL PLCT(4.25,5.25,-3)
20 CCNTINUE
CALL SYMBOL(-4.25,0.,14,TITLE1,0.,19)
CALL PLCT(-4.25,5.,-3)
CALL PLOT
FCRMAT(20A4)
1001 FCRMAT(F10.4,115)
END
C

```

```

CTRP1850
CTRP1860
CTRP1870
CTRP1880
CTRP1890
CTRP1900
CTRP1910
CTRP1920
CTRP1930
CTRP1940
CTRP1950
CTRP1960
CTRP1970
CTRP1980
CTRP1990
CTRP2000
CTRP2010
CTRP2020
CTRP2030
CTRP2040
CTRP2050
CTRP2060
CTRP2070
CTRP2080
CTRP2090
CTRP2100
CTRP2110
CTRP2120
CTRP2130
CTRP2140
CTRP2150
CTRP2160
CTRP2170
CTRP2180
CTRP2190
CTRP2200
CTRP2210
CTRP2220
CTRP2230
CTRP2240
CTRP2250
CTRP2260
CTRP2270
CTRP2280
CTRP2290
CTRP2300
CTRP2310
CTRP2320

```


LIST OF REFERENCES

1. Massachusetts Institute of Technology Report No. 82448-1, A Finite Element Program for Automatic Dynamic Incremental Nonlinear Analysis (ADINA), by K. Bathe, May 1976.
2. Kibler, A. E., A Finite Element Preprocessor for SAP IV and ADINA, M. S. Thesis, Naval Postgraduate School, Monterey, CA, September 1977.
3. Giles, G. L., Digital Computer Programs for Generating Oblique Orthographic Projections and Contour Plots, Document No. N75-17124, National Technical Information Service, U.S. Department of Commerce, January 1975.
4. AIRESEARCH Manufacturing Co. of Arizona, Blade Sections, Rotor, First Stage Turbine, Drawing No. D-TL-3103936, August 1976.
5. AIRESEARCH Manufacturing Co. of Arizona, Blade Turbine Rotor-First State Ceramic, Drawing No. E-99193-3101936, September 1976.
6. AIRESEARCH Manufacturing Co. of Arizona, Dovetail, Blade, Rotor, Drawing No. E-TL-965344, September 1976.
7. Preisel, J., Stress Analysis of Ceramic Turbine Blades by Finite Element Method - Part II, Engineer Thesis, Naval Postgraduate School, Monterey, CA, March 1978.
8. Bathe, K. J. and Wilson, E. L., Numerical Methods in Finite Element Analysis, 1st ed., Prentice Hall, 1976.
9. AIRESEARCH Manufacturing Co. of Arizona, First Design Review Meeting Presentation and Discussion of the Ceramic Gas Turbine Engine Demonstration Program, Report No. 76-211935-15, September 1976.
10. Pratt and Whitney Aircraft Division of United Technologies, Design, Fabrication and Spin Testing of Ceramic Blade-Metal Disk Attachment, Quarterly Report Nos. 1, 2, 3, and 4, Contract NAS3-19715, 1975-1976.
11. Anderson, C. A., Bratton, R. J., Cohn, A., Sanday, S. C. and Lange, F. F., Progress on Ceramic Rotor Blade Development for Industrial Gas Turbines, ASME paper 77-gt-42, Presented at ASME Gas Turbine Conference, 27-31 March 1977, Philadelphia, PA.

12. Naval Postgraduate School Technical Note No. 0141-03,
Plotting Package for NPS IBM 360/67, by Patricia C.
Johnson, August 1977.
13. Naval Postgraduate School Technical Note NO. 0141-28,
Tektronix 4012 Computer Display Terminal with CP/CMS,
User's Instruction Guide, by Richard Donat, May 1974.
14. Tektronix Inc., Plot-10 Terminal Control System User's
Manual, Document No. 062-1438-00, May 1974.
15. Tektronix Inc., Plot-10 Advanced Graphing II User's
Manual, Document No. 062-1530-00, 1973.

INITIAL DISTRIBUTION LIST

	No. Copies
1. Defense Documentation Center Cameron Station Alexandria, Virginia 22314	2
2. Library, Code 0142 Naval Postgraduate School Monterey, California 93940	2
3. Department Chairman, Code 69 Department of Mechanical Engineering Naval Postgraduate School Monterey, California 93940	1
4. Professor Gilles Cantin, Code 69Ci Department of Mechanical Engineering Naval Postgraduate School Monterey, California 93940	12
5. LCDR Lael R. Easterling, USN 4243 N. W. 54th Oklahoma City, Oklahoma 73112	2
6. Georges Verchery Department de Genie Mecanique Universite de Technologie 60200 Compiègne, France	2
7. Jean Louis Armand Institut de Recherche Pour la Construction Navale 3 Avenue de Grand Champ 78230 le Pecq, France	2
8. Prof. K. J. Bathe Mechanical Engineering Department M. I. T. 77 Massachusetts Avenue Cambridge, Massachusetts 02139	2
9. William J. Dodge Oak Ridge National Lab. Building 9204-1 Box Y Oak Ridge, Tennessee 36830	1

	No. Copies
10. Jack Tree Air Research Manufacturing Co. 402 South 36th Street P. O. Box 5217 Phoenix, Arizona 85010	2
11. Prof. Edward L. Wilson Structural Engineering Division Civil Engineering Department University of California (Berkeley) Berkeley, California 94720	1
12. Dr. William J. Stronge (Code 603) Naval Weapons Center China Lake, California 93955	2
13. J. E. Serpanos Code 3162 Naval Weapons Center China Lake, California 93955	1
14. Dr. Jean Louis Batoz, (I-230) Department of Civil Engineering Massachusetts Institute of Technology Cambridge, Massachusetts 02139	1
15. Prof. Guri Dhatt Centre Technique de l'Informatique Universite Laval Quebec, Prov. de Quebec Canada, G1K7P4	1
16. John Fairbanks Department of Energy Division of Power Systems 20 Massachusetts Ave. N. W. Washington, D. C. 20545	1
17. Dr. Gilbert Tougot Centre d'Informatique Universite de Technologie 60206 Compiegne, France	1
18. R. A. Langworthy Applied Technology Laboratories U. S. Army Research and Technology Laboratory Fort Eustis, Virginia 23604	1

	No. Copies
19. E. M. Lenoe Army Materials & Mechanic Research Center Arsenal Street Watertown, Massachusetts 02172	1
20. Dr. Paris Genalis Naval Ship Research and Development Center Bethesda, Maryland 20084	1
21. C. Miller Naval Sea Systems Command Department of the Navy Washington, D. C. 20362	1
22. Code SEC 6734 Naval Ship Engineering Center Philadelphia Division Philadelphia, Pennsylvania 19112	1
23. A. M. Diness (Code 471) Department of the Navy Office of Naval Research Arlington, Virginia 22217	1
24. Ray M. Standahar Office of Secretary of Defense DDR&E 3D1089 Pentagon Washington, D. C. 20301	1
25. R. Rice (Code 6360) Naval Research Laboratory Washington, D. C. 20375	1
26. E. Van Reuth Defense Advanced Research Projects Agency 1440 Wilson Boulevard Arlington, Virginia 22209	1
27. I. Machlin Naval Air System Command Department of the Navy Washington, D. C. 20361	1
28. B. Probst, MS 49-3 NASA-Lewis Research Center 21000 Brookpark Road Cleveland, Ohio 44135	1

	No. Copies
29. Mr. C. P. Blankenship, MS105-1 NASA-Lewis Research Center 21000 Brookpark Road Cleveland, Ohio 44135	1
30. Dr. H. Graham/AFML/LLM Department of the Air Force Air Force Materials Laboratory Wright-Patterson Air Force Base, Ohio 45433	1
31. Mr. George Strong DCASMA, Phoenix 3800 North Central Avenue Phoenix, Arizona 85012	1
32. S. Freiman (Code 6363) Naval Research Laboratory Washington, D. C. 20375	1
33. AFML/LLM/ N. M. Geyer Air Force Materials Laboratory Wright-Patterson Air Force Base, Ohio 45433	1
34. S. Wiederhorn National Bureau of Standards Washington, D. C. 20234	1
35. LT J. H. Preisel, Jr., USN 922 Bernard Road Peekskill, New York 10566	1
36. Allan F. Greiner United Technologies Research Center East Hartford, Connecticut 06108	1